REVEALING LIVESTOCK EFFECTS ON BUNCHGRASS VEGETATION WITH LANDSAT ETM+ DATA ACROSS A GRAZING SEASON

A Thesis

Presented in Partial Fulfillment of the Requirements for the

Degree of Master of Science

with a

Major in Environmental Science

in the

College of Graduate Studies

University of Idaho

by

Vincent S. Jansen

May 2014

Major Professor: Crystal Kolden, Ph.D.

Authorization to Submit Thesis

This thesis of Vincent S. Jansen, submitted for the degree of Master of Science with a major in Environmental Science and titled "Revealing Livestock Effects on Bunchgrass Vegetation with Landsat ETM+ Data Across a Grazing Season," has been reviewed in final form. Permission, as indicated by the signatures and dates given below, is now granted to submit final copies to the College of Graduate Studies for approval.

Major Professor ________________________________Date__________
Crystal Kolden, Ph.D.

Committee
Members ________________________________Date__________
Robert V. Taylor, Ph.D.

________________________________Date__________
Beth Newingham, Ph.D.

________________________________Date__________
J.D. Wulfhorst, Ph.D.

Program
Director ________________________________Date__________
Jan Boll, Ph.D.

Discipline's
College Dean ________________________________Date__________
Paul Joyce, Ph.D.

Final Approval and Acceptance by the College of Graduate Studies

________________________________Date__________
Jie Chen, Ph.D.

Abstract

Remote sensing provides monitoring solutions for more informed grazing management. To investigate the ability to detect the effects of cattle grazing on bunchgrass vegetation with Landsat Enhanced Thematic Mapper Plus (ETM+) data, we conducted a study on the Zumwalt Prairie in northeastern Oregon across a gradient of grazing intensities. Biophysical vegetation data was collected on vertical structure, biomass, and cover at three different time periods during the grazing season: June, August, and October 2012. To relate these measures to the remotely sensed Landsat ETM+ data, Pearson's correlations and multiple regression models were computed. Using the best models, predicted vegetation metrics were then mapped across the study area. Results indicated that models using common vegetation indices had the ability to discern different levels of grazing across the study area. Results can be distributed to land managers to help guide grassland conservation by improving monitoring of bunchgrass vegetation for sustainable livestock management.

Acknowledgements

This research was completed with support from National Aeronautics and Space Administration (NASA) contract number NNX10AT77A; NSF Idaho EPSCoR award number EPS-0814387; NSF GK-12 grant DGE - 0841199; The Nature Conservancy (TNC).

Vital support also came in the form of volunteer labor and vegetation storage. I would like to thank Katie Morrison, Collette Gantenbein, Bill Mathews, Brent Wydrinski, Jerri Moro, Joe Chigbrow, Lydia Bailey, and Lueders and Taylor.

Acknowledgements also must go out to all the faculty, staff and students at the University of Idaho and employees of The Nature Conservancy who assisted in the completion of this research. I would like to thank Beth Newingham, J.D. Wulfhorst, and Crystal Kolden who provided informative reviews, feedback, and support at U of I. I am also thankful to Robert V. Taylor from TNC for all the insightful ideas, advice and reviews over the years and setting this research into motion. Thanks to Jeff Fields from TNC for all the encouragement and logistical support on and off the Zumwalt Prairie Preserve. A special thanks goes out to the PyroGeography lab and Arjan Meddens whom provided valuable assistance on data analysis and manuscript revisions.

Table of Contents

List of Figures

List of Tables

Chapter 1: Revealing Livestock Effects on Bunchgrass Vegetation with Landsat ETM+ Data Across a Grazing Season

Abstract

Proper livestock grazing is vital to maintain grassland ecosystem functioning. Traditional field techniques to monitor grazing are costly and limited to small spatial scales. Remote sensing provides monitoring solutions for more informed grazing management. To investigate the effect of cattle grazing on bunchgrass grassland vegetation, we sampled 32 sites across four prescribed stocking rates on the Zumwalt Prairie in northeastern Oregon; high (1.08 Animal Unit Month per hectare (AUM/HA)), medium (0.72), low (0.36) and control (0). We collected vegetation data on vertical structure, biomass, and cover at three different time periods during the grazing season: June, August, and October 2012. Remotely sensed Landsat Enhanced Thematic Mapper Plus (ETM+) data was acquired closest in date to three field sampling bouts. We correlated the field-observed vegetation metrics (biomass, cover, and vertical structure) to Landsat spectral bands, 14 commonly used vegetation indices, and the tasseled cap wetness, brightness, and greenness transformations. To increase the explanatory value of the satellite derived data, full, step-wise, and best-subset multiple regression models were fit to each of the vegetation metrics at the three different times of year. Predicted vegetation metrics were then mapped across the study area. Field-based results indicated that as the stocking rate increased, the mean vegetation amounts of vertical structure, cover, and biomass decreased. The multiple regression models using common vegetation indices had the ability to discern different levels of grazing across the Pacific Northwest Bunchgrass Prairie. Field measures of vegetation cover yielded the highest correlations to remotely sensed data across all sampling periods. Our results will help guide grassland conservation by improving

monitoring of bunchgrass vegetation for sustainable livestock management on the Zumwalt Prairie.

1. Introduction

The world's grassland ecosystems are of high conservation importance, as nearly half the historic area has been converted to different land use types and less than 5% of what remains falls under conservation protection (Hoekstra et al., 2004). Grasslands provide important forage for the livestock industry and vital habitat for native wildlife (Allen-Diaz et al., 1995; Conner et al., 2002). Due to potential adverse effects incompatible grazing poses to structure and function of grasslands (Johnson et al., 2011; Milchunas and Lauenroth, 1993), wildlife (Johnson et al., 2012; Kimoto et al., 2012), and a rancher's income (Holechek and Gomez, 1999) cost-effective monitoring is needed (Washington-Allen et al., 2006). Accurate, cost-effective monitoring that is quantitative and repeatable across large spatial extents has proven to be difficult with traditional rangeland monitoring techniques (Booth and Tueller, 2003; Pickup et al., 1994; Washington-Allen et al., 2006; West, 2003). Therefore timely monitoring of heterogeneous vegetation across large areas requires new methods and technology (Hunt et al., 2003; Pickup et al., 1994). Recently, focus on quantitative data for management purposes across greater spatial and temporal scales has compelled researchers to turn to remote sensing in order to improve upon existing monitoring datasets (Herrick et al., 2010) and derive empirical, repeatable measures of important grassland vegetation metrics (Marsett et al., 2006; Todd et al., 1998).

Using space-borne remote sensing data helps solve both timing and scale issues associated with vegetation and grazing monitoring, due to repeat visits of satellites and full spatial coverage of Earth. Using satellite data, previous investigators have employed a variety of analysis techniques to quantify common rangeland monitoring metrics, such as vertical structure (Marsett et al., 2006), cover (Blanco et al., 2009; Hagen et al., 2012; Purevdorj and Tateishi, 1998; Röder et al., 2008; Marsett et al., 2006), and biomass (Brinkmann et al., 2011; Todd et al., 1998; Marsett et al., 2006). Field measures are typically correlated to vegetation indices or transformations derived from remotely sensed data (Dungan, 1998) to determine the most applicable index for vegetation monitoring (Zhang and Guo, 2008). Relationships can be modeled between the field data collected at training sites and satellite derived data from the geospatially co-located pixel or window corresponding to that site (Dungan, 1998; Marsett et al., 2006; Vescovo and Gianelle, 2008; Yang and Guo, 2011; Zhang and Guo, 2008). The diversity of grassland vegetation, soil characteristics, and phenological patterns, coupled with a variety of vegetation metrics, creates the need to identify relationships with a wide variety of band data, vegetation indices, and transformations (Todd et al., 1998; Vescovo and Gianelle, 2008; Yang and Guo, 2011; Zhang and Guo, 2008). Once relationships are established between vegetation metrics and remotely sensed data, grazing effects have been quantified in a variety of ways (Kawamura et al., 2005; Pickup et al., 1998; Yang and Guo, 2011). One method is to test the significance of the relationship between set grazing intensities and remotely sensed data or compare the average vegetation index values between pasture areas with different grazing intensities (Numata et al., 2007; Yang and Guo, 2011). Grazing management practices have also been assessed by quantifying the trend in a specific vegetation index across many years (Archer, 2004; Bradley and O'sullivan, 2011; Evans and Geerken, 2004; Hill et al., 1998; Röder et al., 2008; Washington-Allen et al., 2006) or establishing a grazing gradient (Lind and Rasmussen, 2003; Pickup et al., 1994, Pickup et al.,

1998) to quantify how vegetation cover changes with distance from a water source for livestock.

While these approaches provide some understanding of the change in vegetation amounts caused by grazing, remotely sensed products for rangeland management decision-making are still lacking (Butterfield and Malmstrom, 2006; Hagen et al., 2012; Hunt et al., 2003; Marsett et al., 2006; Washington-Allen et al., 2006). Prior studies have measured vegetation mostly during peak greenness (e.g. Brinkmann et al., 2011; Paudel and Andersen, 2010), which may be helpful for long-term trends in condition. However in many grassland systems pastures are grazed after peak greenness theoretically changing vegetation quantities and subsequent metrics used for next year's management action (Hagen et al., 2012; Marsett et al., 2006). Anderson (1993) highlights the need for timely in-season evaluation of livestock use during the grazing season for adaptive decision-making; Holechek (1988) states that many rangeland systems use end-of-year measures to make decisions for next year rotations. Ideally, land managers could track common rangeland vegetation monitoring metrics across the growing season (Marsett et al., 2006) and monitor changes in these metrics with different stocking rates to make more informed decisions during the current grazing period and for the next year. In addition to temporal data needs, remote sensing data must align with the spatial scales at which land management decision are made. Freely available Landsat data at a 30 meter spatial resolution with a 16-day return interval has been shown to be a well suited sensor for rangeland management purposes that provides necessary vegetation monitoring metrics at suitable management scales (Ikeda et al., 1999).

Effects of grazing on trend and condition have been the focus of research on many rangeland sites (e.g., Bastin et al., 2012; Bradley and O'sullivan, 2011; Munyati and Makgale, 2009; Paudel and Andersen, 2010; Pickup et al., 1994; Washington-allen et al., 2006). However, the Pacific Northwest Bunchgrass prairie has yet to be studied for the detection of grazing with remote sensing. This unique grassland habitat has had much of its historic range converted to crop agriculture (Bartuszevige et al., 2012), and has been shown to be sensitive to grazing pressure (Johnson et al., 2011; McLean and Tisdale, 1972; Skovlin et al., 1976). Grazing on this grassland type predominantly occurs in the summer and fall months (Bartuszevige et al., 2012) mostly after peak greenness, providing a good study site to test quantification of grazing effects after peak greenness and across the grazing season. To date, there is no universally accepted remote sensing methodology or vegetation index that provides important grassland monitoring information across the year for timely management decision making. Limited studies have attempted to quantify vegetation amounts across a single grazing season (Marsett et al., 2006) and few studies have tried to quantify vegetation responses to various grazing intensities (Munyati and Makgale, 2009; Numata et al., 2007; Yang and Guo, 2011).

We assessed the utility of moderate spatial resolution Landsat data for quantifying and monitoring three vegetation metrics (i.e., percent vegetation cover, biomass, and vertical structure) associated with grazing on a semi-arid bunchgrass prairie in northeastern Oregon. The goal was to determine if remotely sensed data are sensitive enough to differentiate various levels of grazing intensities. To achieve this goal, we 1) characterized relationships between field-based metrics and grazing rates, 2) quantified relationships between Landsat data and field-based metrics, and 3) assessed the strength of the relationships across the growing season. We hypothesized that if consistent, significant relationships between remotely sensed indices and vegetation amounts exist, one can evaluate how vegetation amounts differ across the landscape and between stocking rates thereby providing management data to help guide more informed and sustainable grazing rotations.

2. Methods

2.1 Study area

The study was conducted on the Zumwalt Prairie Preserve, owned by The Nature Conservancy (TNC) (latitude 45˚33’N, longitude 117˚02’W, elevation 1500m) in Wallowa County, Oregon, USA (Fig. 1). The Zumwalt Prairie Preserve is a small 13,000 hectare section of the bigger Zumwalt Prairie area which is close to 130,000 hectares in size and is dominated by C_3 grasses that include Idaho fescue (*Festuca idahoensis* Elmer), bluebunch wheatgrass (*Pseudoroegneria spicata* (Pursh) A. Love) and Sandberg’s bluegrass (*Poa secunda* J Presl). Average summer (June – August) temperatures range from 11.8 – 17.5˚C, with an average annual precipitation of 348.3mm (2006-2012 Zumwalt Weather Station). The total annual precipitation for 2012 was 14.4 mm below normal, with August and September receiving no measurable precipitation. Although many grassland systems worldwide are now used for crop production, the Zumwalt Prairie largely escaped the plow because of the short growing season and shallow soils (Bartuszevige et al., 2012). Before the area was settled by Anglo Americans, the Nez Perce Tribe (Nimíipuu) grazed horses and cattle beginning in the 1700’s (Bartuszevige et al., 2012). The majority of land currently on the Zumwalt is privately owned and livestock grazing has been the major land use for well over 100 years, with spring/summer pasturing of beef cattle the predominant use in the last half century (Bartuszevige et al., 2012).

2.2 Study design

To define the suitable habitat sampling area, we limited our study to the ecological systems “Columbia Basin Palouse Prairie” and “Columbia Basin Foothill and Canyon Dry Grassland” as defined by the ReGap Ecological Systems data (ONHIC, 2006). To reduce spectral noise from path radiance and shadowing of slopes, survey sites were located in areas with less than 30% slope and at least 50m away from roads, stock ponds, and fence lines, and at least 200m from other field sites.

Grazing treatments were prescribed by TNC land managers to align with prior grazing studies on the Zumwalt Prairie (Johnson et al., 2011). The pastures were stocked at four different rates high (1.08 Animal Unit Month (AUM)/HA), medium (0.72), low (0.36) and control or no use by livestock (0)). Field data was collected in three different sampling bouts: June 26 – July 4, August 10 – 16, and September 27 – Oct 5, 2012 (Fig 2). Thirty-two sites across three different stocking rates were sampled in each bout. Sample sites were chosen within areas of homogenous vegetation to best represent a gradient of vegetation amounts (e.g. Wylie et al., 2002). Twelve sampling sites were placed in pastures with a high stocking rate, ten sites in pastures with a medium rate and ten in control (No Graze) pasture areas (Fig 2). Due to limited resources and time no sites were monitored within the pastures with low stocking rates.

2.3 Biophysical vegetation measures

At each sampling site a 30m x 30m macroplot was established with two 30 meter transects intersecting plot center aligned in north/south and east/west cardinal directions. Within each macroplot, data on vegetation structure, foliar cover, ground surface, and biomass was collected at three times during the grazing season. Vegetation structure data was collected every five meters from opposite cardinal directions along the two transects following Robel et al. (1970) for a total of 13 measures per macroplot. Cover data (foliar cover, soil surface, and foliar color (green vs. brown)) was collected every meter on each transect using the line-point intercept method (Herrick et al., 2005). Biomass was measured by clipping vegetation within two 0.5 m x 0.5 m quadrats per transect to 0.5 cm above ground surface. Biomass was separated into green (live) and brown (senescent) vegetation and weighed in the field to obtain a wet weight. To obtain dry weight, clipped vegetation placed in an oven at 60°C for 24-36 hours until the weight remained stable. The final weight of the each sample was averaged by macroplot and used as the measure of dry biomass.

2.4 Utilization measure

Assessment of grazing can be performed with a measure of utilization at the end of year, providing information on how much vegetation has been consumed or destroyed by livestock (Coulloudon et al., 1999). Utilization was ocularly estimated at each macroplot during the last sampling bout in October using a double weight sampling method described by Parsons et al. (2003). The average utilization per macroplot was computed by taking the average percent utilization estimated across 10 randomly placed 0.25 m x 0.25 m quadrats. To account for estimate bias, observers first estimated utilization amounts (0% - 100%) in fifteen 0.25 m x 0.25 m calibration quadrats, each of which had varying amounts of vegetation removed to mimic different utilization rates prior to sampling. After the observer estimated utilization, the residual vegetation was clipped to within 0.5 cm of the ground and weighed. The initial clipped vegetation weight was then divided by the total weight (initial + final clipped weight) of the vegetation within the quadrat to obtain utilization (Parsons et al., 2003). For each observer, regression equations were constructed by regressing estimated utilization against the actual utilization (e.g. Parsons et al., 2003). Observer one's regression equation was Y = 0.8513x + 2.880 with $R^2 = 0.61$ and $p = 0.001$; observer two's regression was Y = 1.11999x - 1.9883 with $R^2 = 0.81$ and $p < 0.001$. These equations were then used to correct the observers' estimated utilization for each sample obtained at each macro plot.

2.5 Remotely sensed data

We acquired 11 Level 1 terrain-corrected (LT1) Landsat Enhanced Thematic Mapper-plus (ETM+) scenes for 2012 from WRS-2 path/rows 42/28 and 43/28. Each scene was processed to at-surface reflectance following Chander et al. (2009) and atmospherically corrected using dark object subtraction (Chavez, 1996). Mean at-surface reflectance for each band was then computed using a 2 x 2 pixel window average to fully cover each macroplot. Band data and vegetation indices were then computed for each site using the averaged values for each band.

Landsat data closest in date to the field data collection was attributed to each site for each sampling bout. For sites falling within 'no data' lines associated with the Landsat 7 scan line corrector error (Wulder et al., 2011) or obscured by cloud cover, data were utilized from the next closest scene-date containing valid data. From these reflectance data, vegetation indices and transformations were computed for each sample site for each sampling bout (Fig. 3).

2.6 Vegetation indices

At-surface reflectance data from Landsat ETM+ bands 1-5 and 7, as well as 14 vegetation indices and the tasseled cap transformations (Kauth and Thomas, 1976), were used to estimate relationships with biophysical vegetation data (Table 2). Vegetation indices calculated were the Simple Ratio (SR; Jordan, 1969), Normalized Difference Vegetation Index (NDVI; Rouse et al., 1973; Tucker, 1979), Soil Adjusted Vegetation Index (SAVI; Huete, 1988), Renormalized Difference Vegetation Index (RDVI; Haboudane, 2004; Roujean and Breon, 1995), Modified Triangular Vegetation Index 1 (MTVI1; Haboudane, 2004), Canopy index (CI; Vescovo & Gianelle, 2008), Normalized Canopy Index (NCI; Vescovo and Gianelle, 2008), Ratio Cover Index (RCI; Zhang and Guo, 2008), Normalized Difference Cover Index (NDCI; Zhang and Guo, 2008), Plant Senesce Reflectance Index (PSRI; Merzlyak et al., 1999), Soil Adjusted Total Vegetation Index (SATVI; Marsett et al., 2006), the Seven/Four ratio (7/4), Normalized Difference Infrared Index Seven (NDII7; Hardisky et al., 1983; Key and Benson, 2006), Normalized Difference Water Index (NDWI; Hardisky et al., 1983; Gao, 1996), and the tasseled cap transformations (Kauth and Thomas, 1976) greenness (TCGRE), brightness (TCBRI) and wetness (TCWET) (Table 3).

These vegetation indices were selected based on prior research performed on other grasslands (Marsett et al., 2006; Numata et al., 2007; Yang and Guo, 2011; Zhang and Guo, 2008). Vegetation indices that incorporate red (band 3) and near-infrared (band 4 (NIR)) bands have been shown to be effective at measuring green vegetation amounts by differencing the reflectance values between the near-infrared and red portion of the electromagnetic spectrum (Marsett et al., 2006; Rouse et al., 1973; Tucker, 1979). Indices that incorporate the shortwave-infrared bands (Band 5 (SWIR1) and band 7 (SWIR2)), which are sensitive to water content, have been shown to provide good measurements of both green and senescent vegetation quantity (Hardisky et al., 1983; Marsett et al., 2006; Numata et al., 2007; Pickup et al., 1994; Yang and Guo, 2011). Vegetation indices that incorporate the shortwave-infrared band 7 in combination with the NIR band have typically been used for forest disturbances, such as fire, and can be used to differentiate live vegetation from soil, ash, and burned vegetation (Key, 2006). The tasseled cap transformation is a linear combination of 6 spectral bands of Landsat ETM+ data that results in three images of wetness, greenness, and brightness that have been shown to be useful in image analysis of agricultural and forested systems (Crist and Kauth, 1986; Kauth and Thomas, 1976).

2.7 Analysis

All biophysical vegetation and remotely sensed data was tested for normality using the Lilliefors test (Lilliefors, 1967). Non-normal data distributions were normalized and Pearson's correlations were computed between the utilization at each site and the vegetation metrics of vertical structure, biomass, and foliar cover for each sampling bout. Pearson's correlations were also performed between all the remotely sensed data and vertical structure, cover, and biomass for each sampling bout. Correlations with p values less than or equal to 0.05 were considered significant.

To increase the potential predictive power of satellite data to explain the variance of the vegetation metrics, multiple regression techniques were employed. Following Hudak et al. (2006), full, stepwise, and best subset models were created to determine the best predictor variables to model structure, cover, and biomass for each sampling bout. Using both the stepwise and best subset modeling techniques helps to ensure multiple models were explored for the best fit by searching different pathways for variable selection (Hudak et al., 2006). We used a stepwise technique that selects the model with the lowest Akaike Information Criterion (AIC) (Akaike, 1974) by searching both forward and backward pathways (Hudak et al., 2006). Next, a best-subsets method was performed to search all possible pathways, choosing the best variables for a defined number of predictor variables (Hudak et al., 2006). Models with the lowest corrected AIC (Sugiura, 1978) having a variance inflation factor (VIF) less than 10 (Friendly and Kwan, 2009) were selected as the "best" models. We further tested all residuals for a normal distribution with a mean of zero and for spatial auto-correlation using Morans's I (Cliff and Ord, 1981, Todd et al, 1998).

Using the selected regression models we then computed and mapped the estimated cover, biomass, and stucture metric for each Landsat grid cell for each sample bout across the study area. This produced three maps for each vegetation metric; one map representing each of the three sampling bouts (Figs. 4-6). Comparisons of mean estimated vegetatation amounts of cover, biomass, and structure by stocking rate (control, low, medium and high) and sample bout, was performed by bootstrapping the data with replacement 1000 times. To build a 95% confidence interval for the mean value, the 2.5 and 97.5 percentiles were selected. Where confidence intervals around the mean vegetation value for each stocking rate did not overlap, significant differences existed at the 95 % confidence level. To quantify the effects of stocking rate on predicted vegetation, Ordinary Least Square (OLS) regression was performed using the pasture stocking rate (AUM per hectare) as the predictor variable and mean vegetation amount by pasture as a response variable. The slope of each OLS regression indicates the effect stocking rate has on each vegetation amount.

3. Results

3.1 Data exploration of biophysical variables

Utilization ranged from 0 - 35% (Fig 4A). There were no significant differences in utilization between high and medium stocking rates (p value = 0.38). Utilization rates in high and medium treatment pastures were significantly higher than control pastures ($p < 0.001$) (Fig. 4B). Grazing utilization was negatively correlated to all three vegetation metrics across all sampling bouts (Fig. 5). Utilization was most strongly correlated with cover during sampling bout 2 (r = -0.71). Relationships between structure and utilization varied the least across the three sampling periods with r values from -0.59 to -0.62. The biomass vegetation metric had the weakest correlations to utilization, with decreasing relationships observed later in the growing season (Fig. 5).

3.2 Relationships between structure, cover, and biomass with satellite data

The relationships between the biophysical data and satellite indices had r values ranging from -0.75 to +0.74. Band 7, the seven/four ratio and NDII7 were consistently significantly correlated across the growing season to structure (Table 3), canopy cover (Table 4) and biomass (Table 5). The strongest relationships were between cover and the seven/four ratio and NDII7 vegetation indices, all having r values > 0.63 (Table 4). The relationships between the satellite data and biomass and structure also had significant relationships but were more weakly correlated than for cover. For structure Band 7 and the seven/four ratio had the highest correlations, with r values ranging -0.44 to -0.58 across the sampling bouts. Biomass was most correlated to the seven/four ratio or NDII7, having similar results to vertical structure (r values ranging from -.52 to 0.65) in each sample bout across the growing season.

3.3 Multiple regression modeling

Fitting the full, stepwise and best subset models to the biophysical vegetation metrics for each sample bout revealed multicollinearity with the predictor variables. The full model and stepwise models had higher R^2 values and lower corrected AIC values than the best subset models, but the predictor variables were highly collinear. The best subsets models exhibited decreased adjusted-R^2 values when compared to the full and stepwise, but met the assumption that the predictor variables are independent and were therefore more appropriate models (Table 6-8). Each selected best subset ordinary least squares model had normally distributed residuals with a mean of zero and exhibited no significant spatial autocorrelation when tested with Moran's I (Cliff and Ord, 1981; Todd et al., 1998).

The best subset models had statistically significant ($p \leq 0.01$) relationships between satellite data and biophysical data estimates. While all models were statistically significant, the coefficient of determination (R^2) was wide ranging and below 0.7 for all subset models selected. The best subset regression models for structure and biomass had an explained variance that decreased with each successive sampling bout as the growing season progressed and the grassland senesced. The selected models' adjusted-R^2 values for structure estimation decreased from 0.699 in sampling bout 1 to 0.389 in sampling bout 3, while the biomass estimation across the sampling bouts decreased from 0.674 in sampling bout 1 to 0.346 in sampling bout 3. The selected best subset models for cover performed better across the growing season having an adjusted-R^2 greater than 0.60 for each sampling bout (Fig. 6). Using the best model for each sampling bout to predict the vegetation amount collected during any other other sampling bout indicates that no single model could achieve the best relationship across the growing season (Fig. 6). For example, the adjusted-R^2 value decreased when using the best subset model selected for cover during sample bout 1 to model cover for sampling bout 3 from 0.67 to 0.50.

3.4 Sensitivity to stocking rate

Using the best subset models, statistical differences existed between the predicted vegetation amounts by stocking rate that were mapped (Fig. 7-9) across the study area (Fig. 10). Control pastures had significantly higher predicted structure, cover, and biomass compared to medium and high stocking rates; high stocking pastures had the smallest predicted vegetation amounts across all sampling bouts. The treatment area stocked at low and medium rates largely had mean predicted vegetation quantities falling between the high and control treatment means across the growing season. In sampling bout one, the medium stocking rate treatment area had higher predicted vegetation amounts for structure and biomass than the low treatment area, but then switched places having lower predicted vegetation amounts for sampling bout 2 and 3. This is likely attributed to the timing of grazing in one of the medium pastures happening during and after sampling bout one. Estimation of vegetation amounts by stocking rate indicated a significant trend in reduction of vegetation amounts across the gradient of stocking rates (Fig. 11-13). This reduction in vegetation is subsequently observed across all bouts. Depending on time of year for each extra AUM per hectare, biomass was reduced between a range of 65 g per m^2 (sampling bout 1) to 38 g per m^2 (Sampling bout 3) (Fig. 11). The reduction of cover across the grazing gradient was more consistent across the growing season with a measure of around 12% with each AUM per hectare (Fig. 12). Vertical structure was also reduced between 0.18 and 0.30 decimeters with 1 AUM per hectare increase in grazing intensity depending on the time of measurement with the greatest reduction observed in the first sampling bout (Fig. 11).

4. Discussion

Analysis of vegetation amounts across the growing season showed reduced vegetation in areas with greater stocking rates. These findings provide evidence that our remote sensing based models were sensitive enough to discern different levels of stocking rates within the grazing season. However, the models most strongly correlated to vegetation metrics changed over the course of the growing season, suggesting that there is was no temporally consistent best model approach to monitor grazing effects utilizing the remotely sensed indices tested in this grassland system. Creating models that use vegetation indices and bands that most appropriately match up with phenological timing improved a model's ability to explain the ground surface conditions.

Relating our field measures of vertical structure, cover, and biomass with grazing intensity as measured by end of year utilization was performed to validate that vegetation amounts changed with increased stocking rates. Finding significant correlations between our vegetation metrics and utilization metric helps clarify that our models can be used to quantify changes in vegetation due to grazing and not just loss due to changes in phenology and non-herbivory related defoliation. From these data we observed significant negative correlations between vegetation metrics across the grazing season and utilization. Our result showing that vertical structure is sensitive to utilization corroborates Johnson et al. (2011) finding that vegetation structure was significantly reduced with increased grazing intensity in treatment years, as well as one year after grazing. Cover and biomass were also negatively correlated in all sample bouts providing evidence that grazing affects vegetation amounts across the growing season.

Both the Pearson's correlations and the multiple regression models between vegetation data and remotely sensed data indicated that vegetation indices with bands four and seven were the most useful to explain our biophysical vegetation measurements. When performing the Pearson's correlation, the band seven/four ratio and NDII7 best predicted vegetation monitoring metrics across the growing season. Vegetation indices that included band 7 were most often selected using the subset regression approach when finding the "best" models. One explanation is that band 7 is sensitive to soil and vegetation moisture; greater reflectance occurs when plants and soils are dry and more bare ground is present (Knipling, 1970; Tucker, 1980). Band 7 may be indicative of grazing levels and resulting impacts on amount of bare ground and vegetation moisture, with higher grazing intensities creating dryer barer areas.

NDVI had high r values (r>0.7) for green vegetation and green cover but lacked strong correlations with the selected biophysical variables throughout the year as vegetation senesced. Numata et al. (2007) found similar results when assessing vegetation parameters during the dry season in Brazil, finding vegetation indices using band 5 and 7 outperformed NDVI and SAVI.

Over the grazing season, models created using the best subset approach decreased in explanatory power, though remained statistically significant. Cover was the biophysical metric that had the greatest explained variance across the growing season using both Pearson's correlations and the best subset regression models. Therefore, a measure of cover could be the most useful metric for setting management objectives or performing multiyear trend analysis. Cover has also been found by others to be a reliable measure when assessed by satellite (Booth and Tueller, 2003). This research approach also shows that end year vegetation quantity metrics of biomass and vertical structure are more difficult to estimate when vegetation has senesced. If land managers feel the models are not accurate enough to base management decisions off of these relationships, other analysis techniques may be needed. Numata et al. 2007 found that using fraction images of non-photosynthetic vegetation produced from Multiple Endmember Spectral Mixture Analysis (MESMA) (Roberts, Smith, & Adams, 1993) had the best correlation to senescent vegetation. Ideally, one vegetation index would provide all the needed information to monitor the selected biophysical metric across the year (Marsett et al., 2006), but the best subset model selection showed that accuracy is improved by producing models that match phenological ground conditions.

Our ability to explain the field metrics with remote sensing data decreased later in the season. This could be due to (1) vegetation senescence, impacting many of the green vegetation indices, and (2) biophysical data becoming more similar over the course of the growing season, reducing the range of vegetation amounts that is being modelled. With increasing similarity and the amount of variance to be explained decreasing, coupled with a small sample size (n=32) for each sampling bout, the statistical measures become less robust later in the year. Hardisky et al. (1983) and Schino et al. (2003) also found it more difficult to measure biomass later in the year, which they attributed to the reduction of live to dead biomass.

While our study highlights the ability to monitor grazing effects by satellite, it has limitations. First, our highest utilization rate at any given site was just over 35%, a rate not considered high for the Zumwalt Prairie habitat (Holechek and Gomez, 1999; Skovlin et al., 1976). Therefore, the models created in this study to estimate vertical structure, biomass, and cover are best suited for moderate levels of grazing and would likely be improved with more variance in grazing levels. Future studies would benefit from sampling sites with higher amounts of utilization across the landscape. Second, field parameter estimation of biomass was difficult in such a highly heterogeneous landscape. Estimation could be improved with more sub-samples within the 30 x 30 macro plot or a different technique of infield estimation of biomass. Other studies have sampled larger areas in the field; for example, Marsett et al. (2006) had field sites of 90m X 150m helping to ensure the field sampled data was co-registered to only pixels within the field sample area. Lastly, due to year-to-year variations in phenology and production as a result of climate and seasonality of precipitation, collection of data across multiple years, as well as more sampling sites across a greater area of the Zumwalt prairie, would improve our confidence in the models ability to predict vegetation metrics at different times of the grazing season for any given year and place.

5. Conclusions

Rangeland managers need timely and accurate landscape scale estimates of vegetation amounts to determine the effects of their land management decisions. Quantifying common rangeland metrics across a grazing season provides spatially explicit maps and data to land managers for more informed decision making. Marsett et al. (2006) points out that maps derived from remote sensing that quantify vegetation can then be analyzed at different scales with Geographical Information System (GIS) tools. Here we computed the mean vegetation amounts by stocking rate treatment and pasture, but these metrics could be calculated at the ownership level or inside key areas within a pasture. Instead of using maps representing a vegetation index such as NDVI as a proxy for a commonly used rangeland metric, it was also our goal to produce maps that were converted back to the common rangeland management metric desired (i.e. cover, biomass, and vertical structure). This may provide more intuitive and accessible remote sensing products to landowners and managers for decision making, as well as integration of data into other ground based datasets.

Here we explored the ability of freely available satellite data to monitor grazing effects with the goal of providing improved decision-support data for grazing management. We attempted to maximize our ability to accurately model vegetation at different time periods across the grazing season. Though significant relationships between remotely-sensed and biophysical field data were only moderately strong and varied across the three sampling periods, our findings suggest that the effects of different levels of stocking rate can be modeled via Landsat ETM+ data across the grazing season with an acceptable accuracy. Being able to monitor the effects of grazing across the landscape can provide data to better inform land management across the Zumwalt grassland.

Figure 1. Map of study area in the Zumwalt Prairie, Oregon.

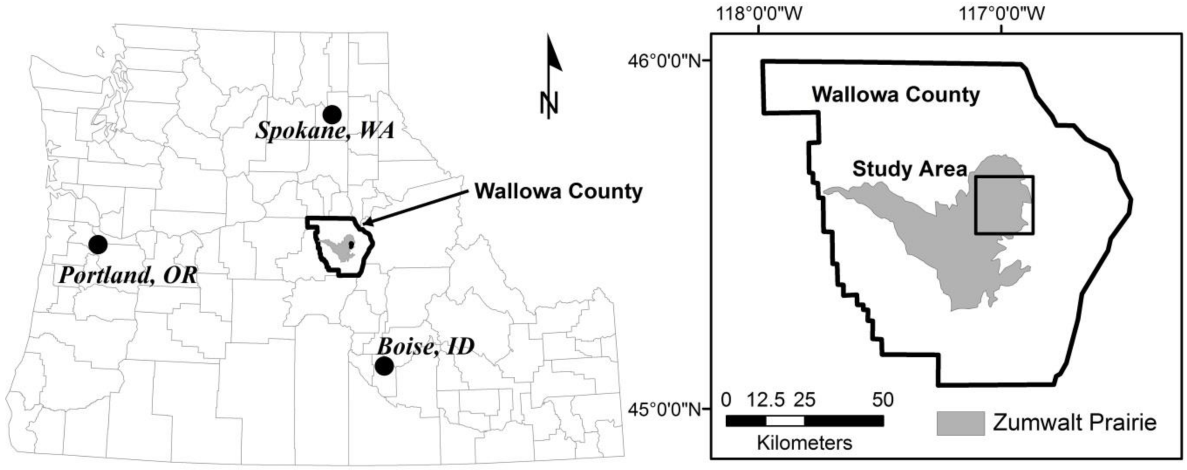

Figure 2. Grazing treatment map showing livestock stocking rates, timing of grazing and location of sites sampled within each pasture. Suitable habitat is delineated using two ecological systems "Columbia Basin Palouse Prairie" and "Columbia Basin Foothill and Canyon Dry Grassland" from ReGap (ONHIC, 2006) and the areas with less than 30% slope, at least 50m away from roads, stock ponds, and fence lines.

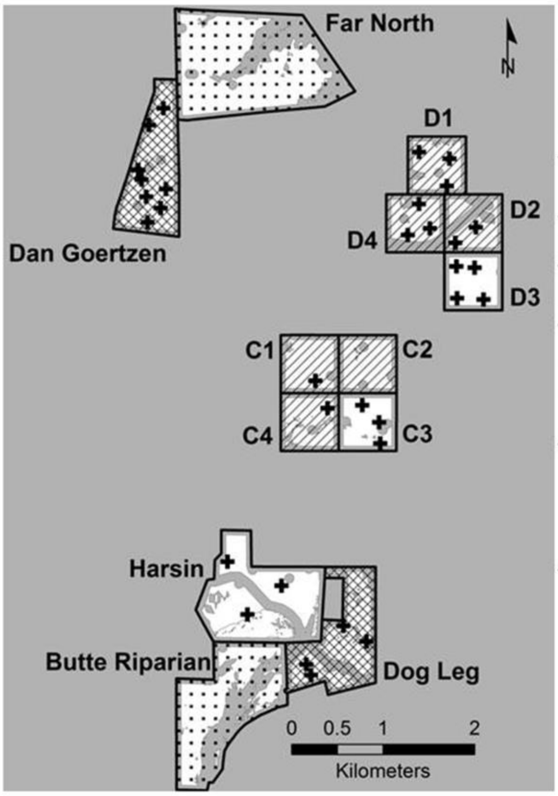

✚ Macroplot
Suitable Habitat
Zumwalt Prairie

Stocking Rate	Pasture/s	Dates Grazed	N
Control - 0 AUM/ha	C3, D3, Harsin	No Graze	10
Low - 0.36 AUM/ha	Far North, Butte Riparian	June 1 – June 23	0
Medium - 0.72 AUM/ha	C1, C2, C4	June 16 – Aug. 4	10
	D1, D2, D4	May 31 – June 22	
High - 1.08 AUM/ha	Dan Goertzen	May 28 – June 21	12
	Dogleg	May 28 – June 11	

Sampling Dates

June 26 – July 4
August 10 – August 16
September 27 – October 5

Figure 3. The timing of the three sampling bouts (the numbered black boxes) in relation to Landsat ETM+ scenes used in the analysis process shown as dates in 2012, as well as the timing of livestock grazing grouped by intensity represented by black lines.

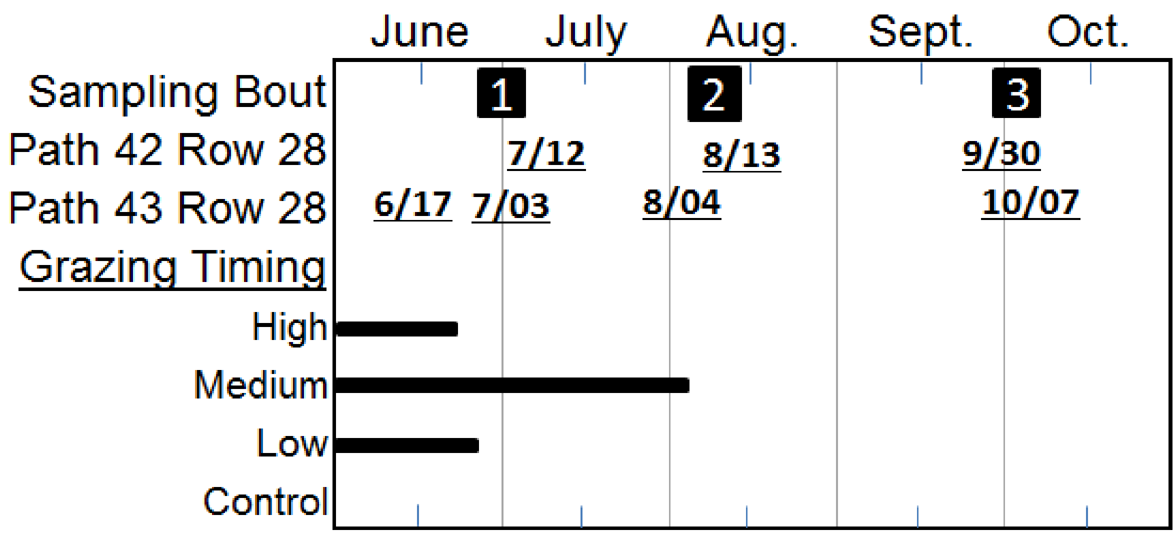

Figure 4. A) Sorted utilization measures collected during the last sampling bout (September 27 – Oct 5) on the Zumwalt Prairie. B) Boxplots of percent utilization by grazing treatment, significant differences exist between the control plots and medium and high grazing treatments, indicated by the different symbols.

A

B

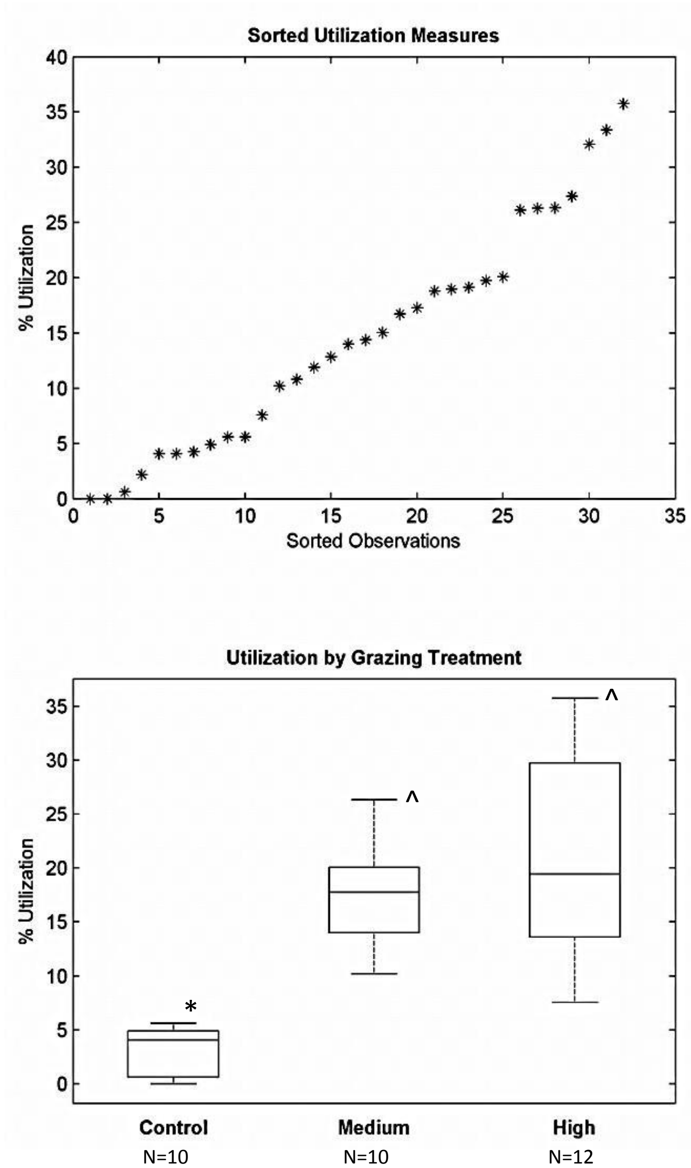

Figure 5. Pearson's correlations between end-of-year percent utilization and biophysical monitoring metrics: vertical structure (dm), cover (%), and dry biomass (g/m2).

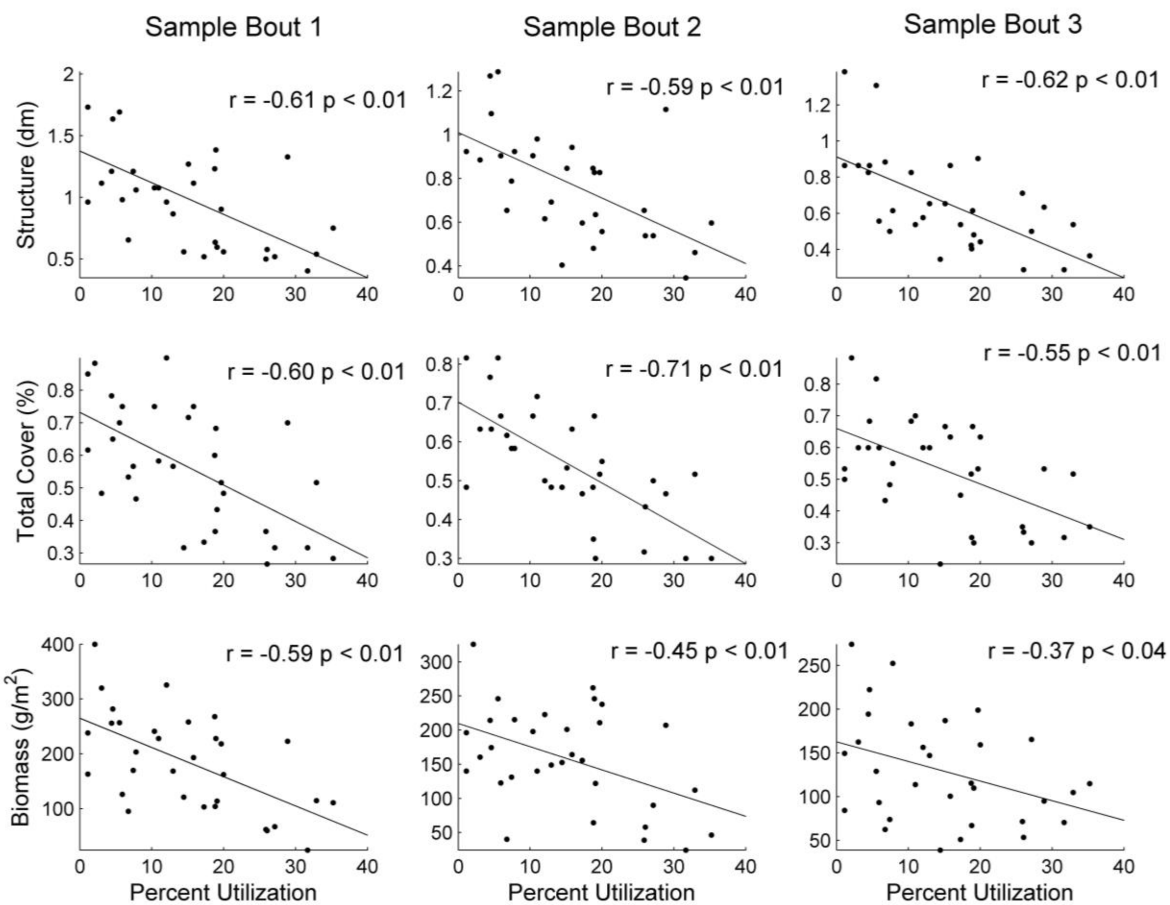

Figure 6. Adjusted R^2 values for the best model regressions for each sampling bout and vegetation metric. The best model from each sampling bout is then used to predict the vegetation metric at the two other sampling bouts.

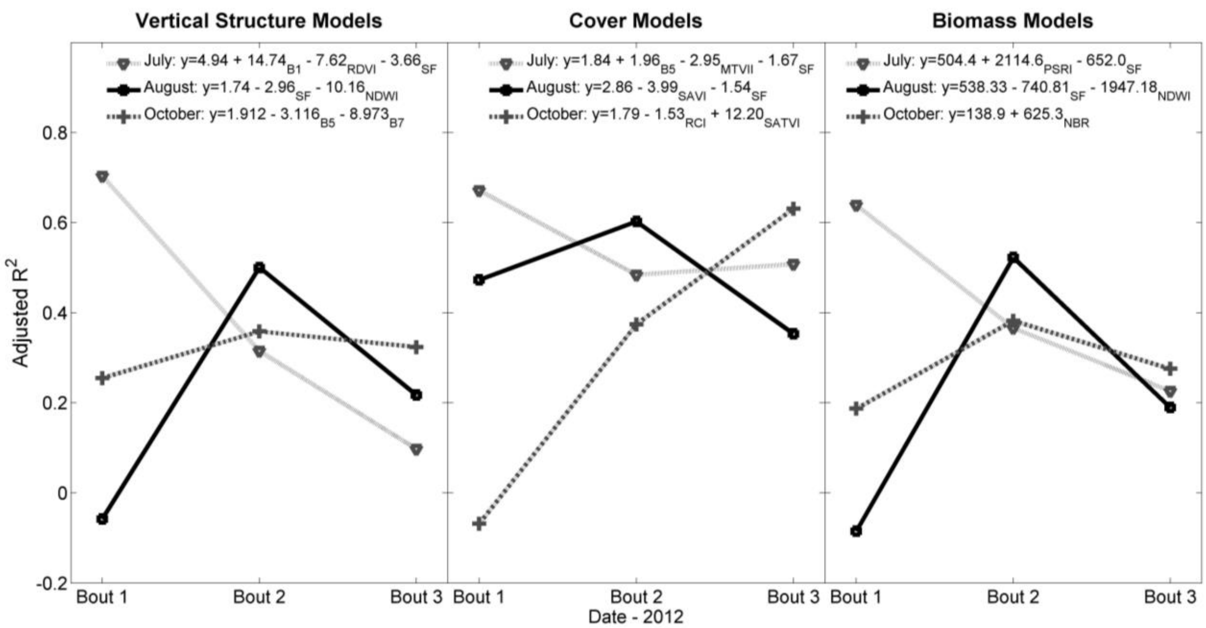

Figure 7. Maps of vegetation structure (dm) by sampling bout and treatment type. No data or values outside of the regression equation range of estimation are shown in red.

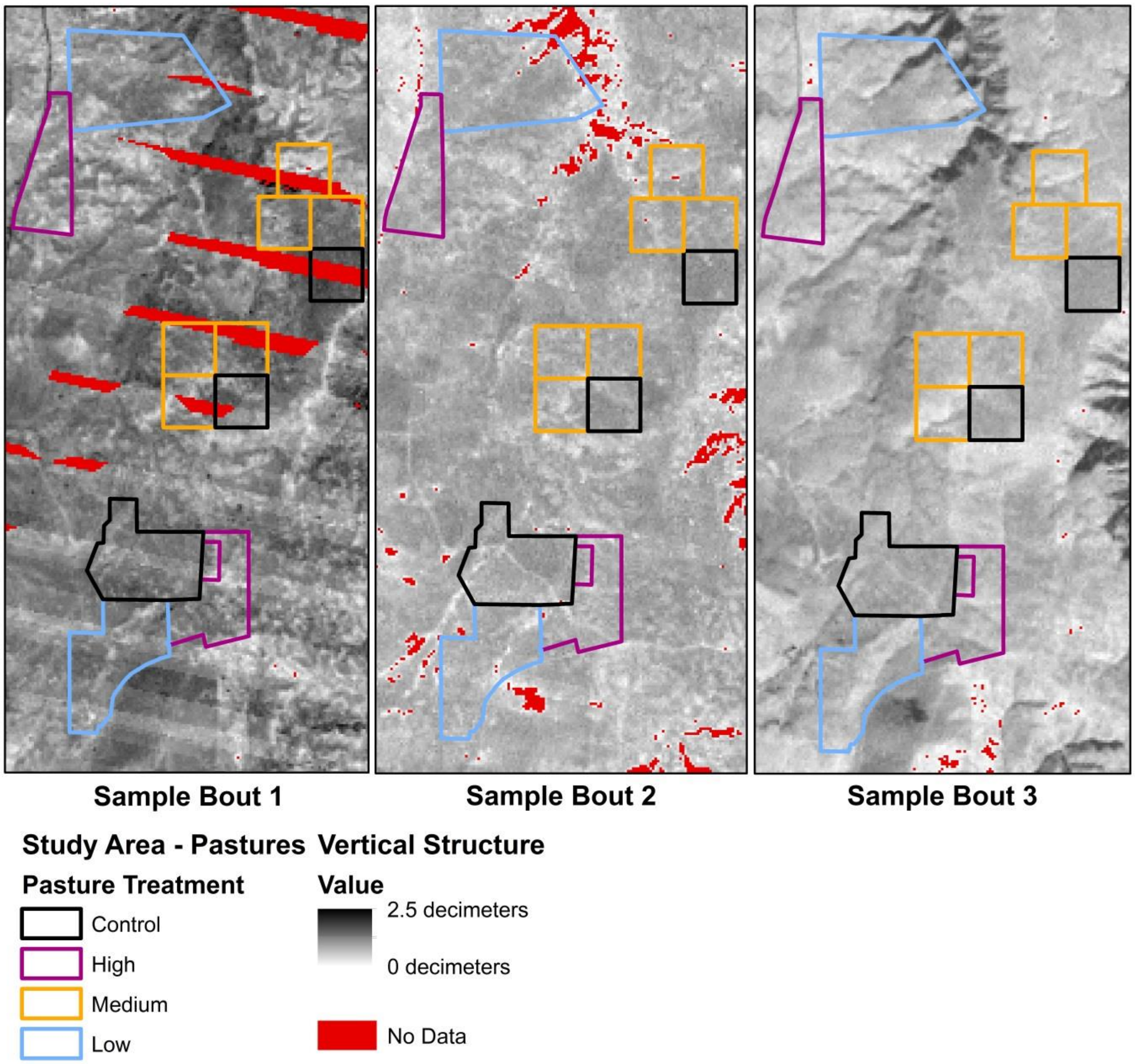

Figure 8. Maps of vegetation cover (%) by sampling bout and treatment type. No data or values outside of the regression equation range of estimation are shown in red.

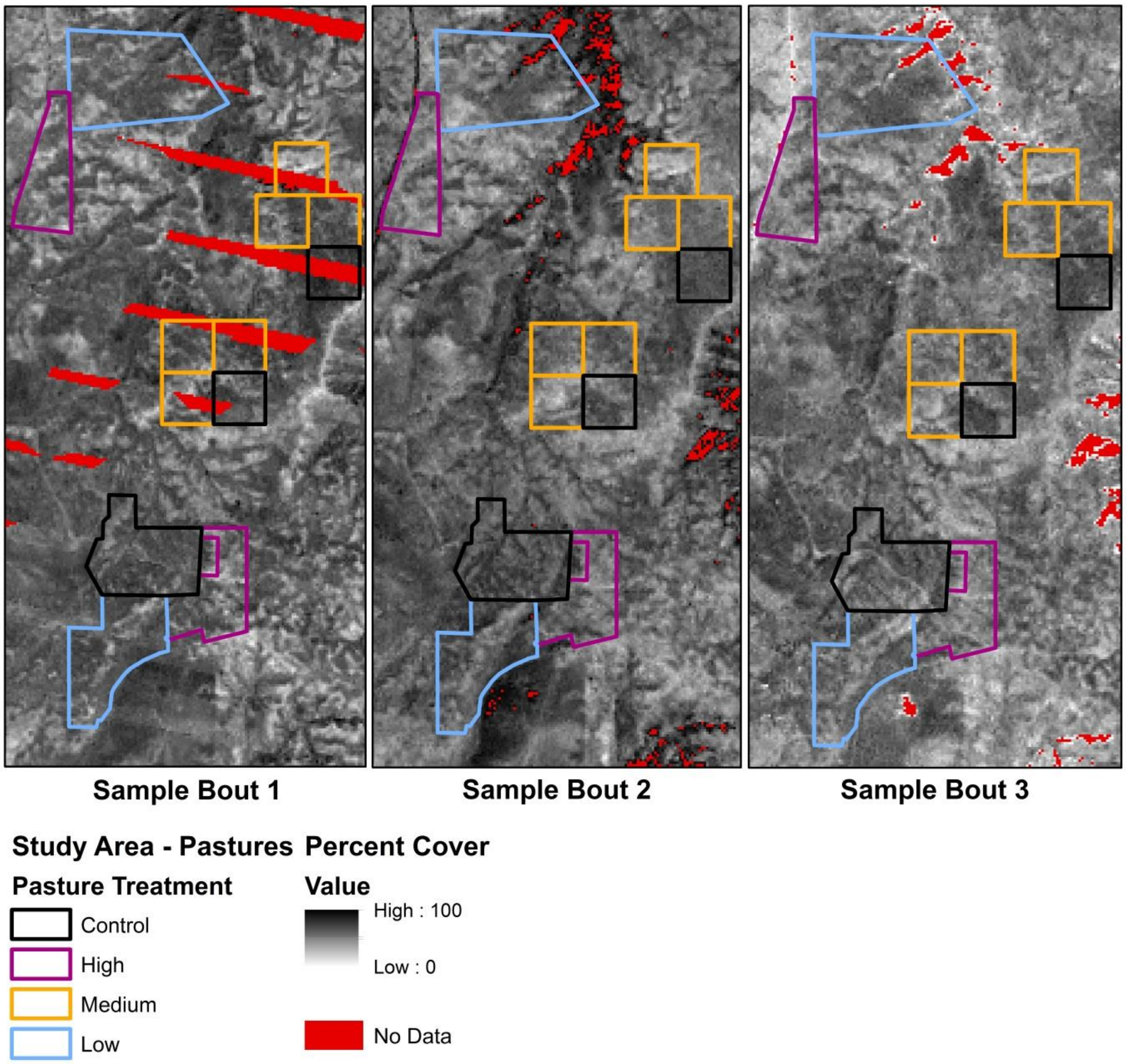

Figure 9. Maps of vegetation biomass (g/m2) by sampling bout and treatment type. No data or values outside of the regression equation range of estimation are shown in red.

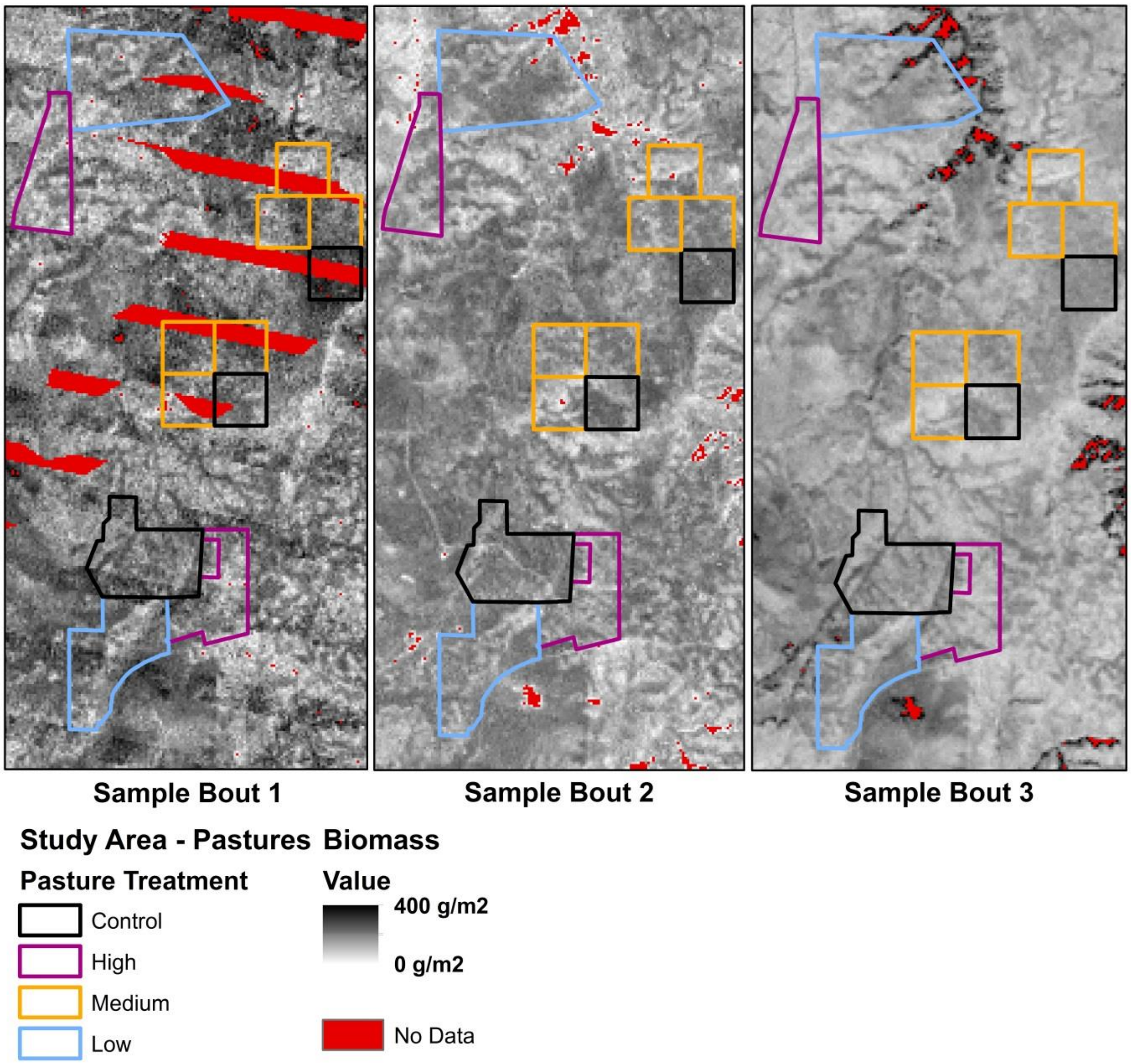

Figure 10. Predicted vegetation amounts for structure, cover, and biomass across the growing season. Means are shown with solid lines, with the filled shaded area showing the 95% confidence interval around the mean. Predicted vegetation amounts were derived from multiple regression analysis by stocking rate and sample bout.

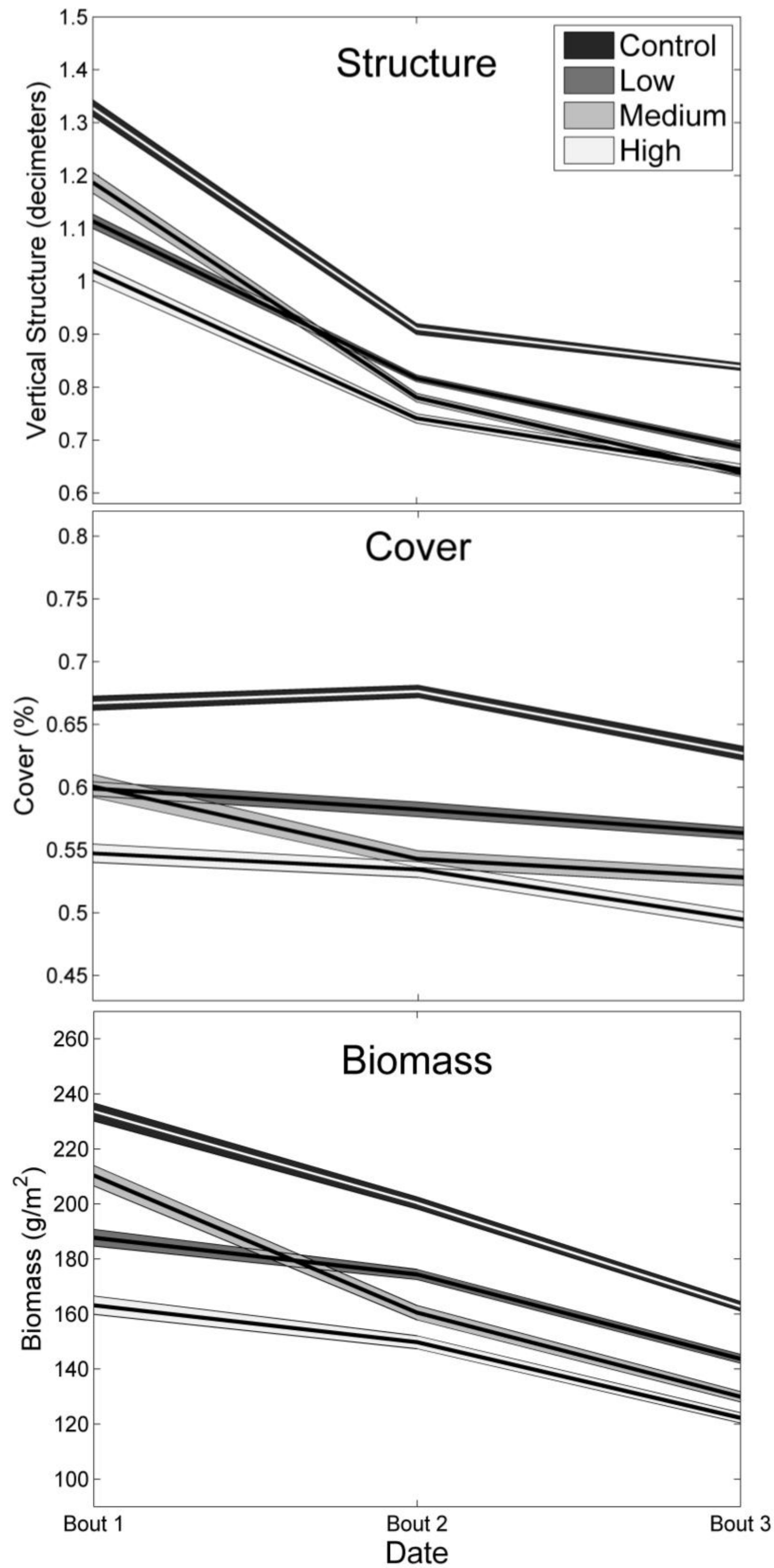

Figure 11. Effect of stocking rate on vertical structure by sampling bout. The point symbols represent the vertical structure (dm) pasture means symbolized by sampling bout. The Ordinary Least Square (OLS) regression lines show the effect of the stocking rate (AUM per hectare) on the mean vertical structure by pasture for each sampling bout The black line and black symbol refer to sampling bout one (SB1) data; the blue line and plus symbol refer to sample bout two (SB2) data; the red line and astrick refer to sampling bout three data (SB3) data.

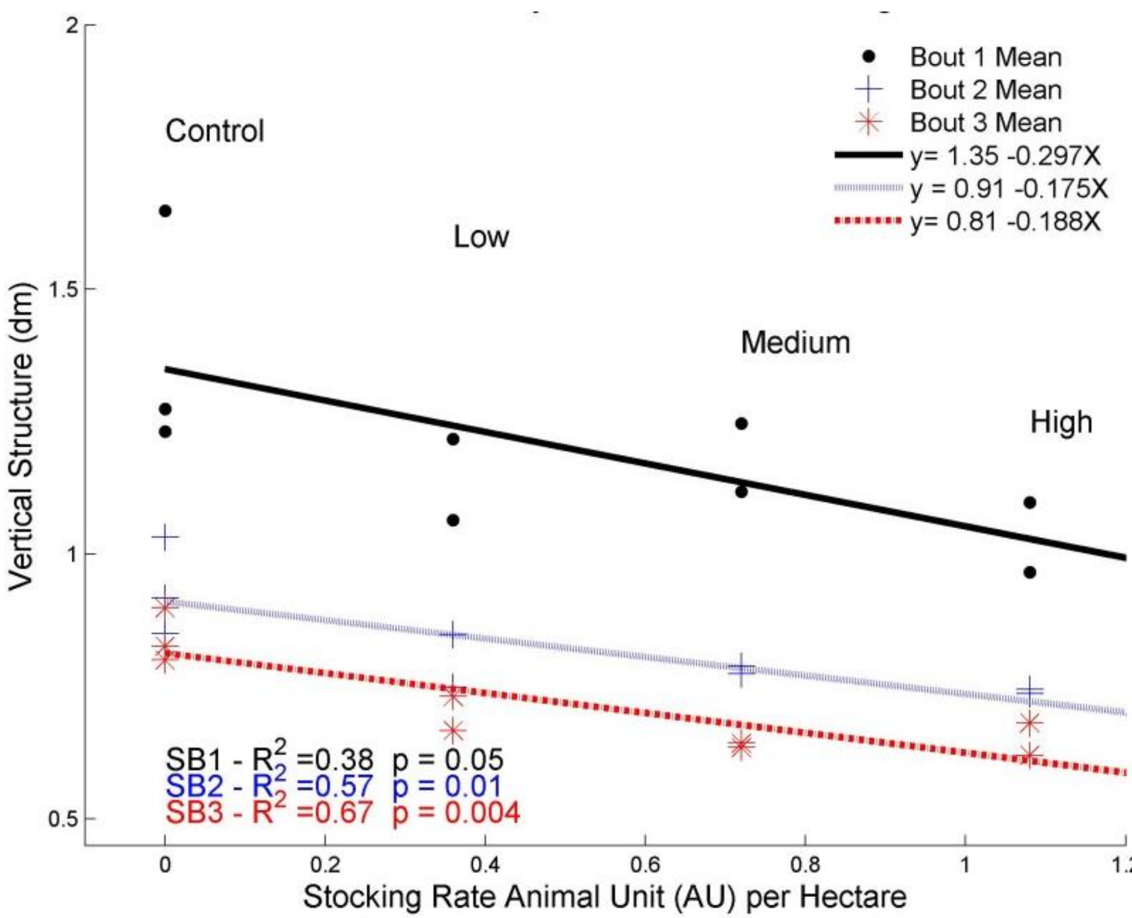

Figure 12. Effect of stocking rate on cover by sampling bout. The point symbols represent the percent cover pasture means symbolized by sampling bout. The Ordinary Least Square (OLS) regression lines show the effect of the stocking rate (AUM per hectare) on the mean percent cover by pasture for each sampling bout. The black line and black symbol refer to sampling bout one (SB1) data; the blue line and plus symbol refer to sample bout two (SB2) data; the red line and astrick refer to sampling bout three data (SB3) data.

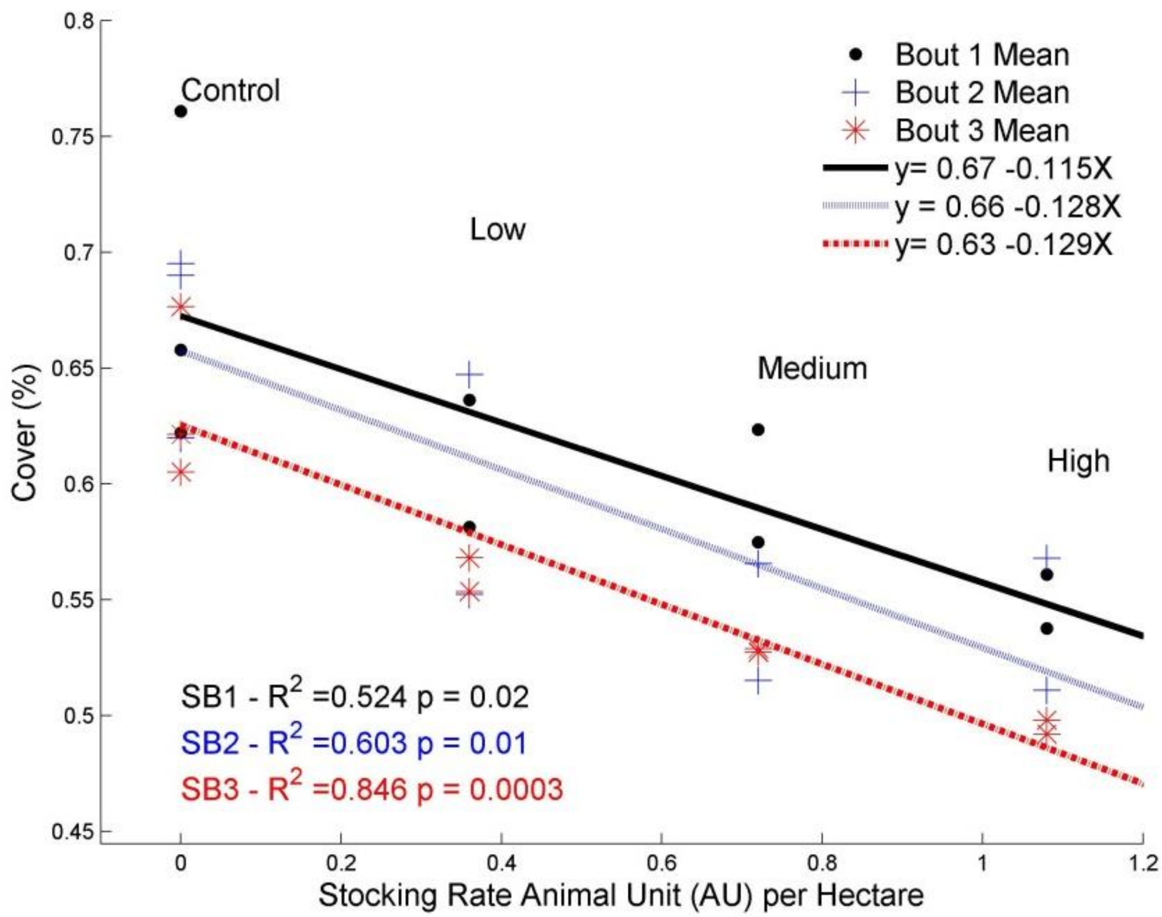

Figure 13. Effect of stocking rate on biomass by sampling bout. The point symbols represent the biomass (g/m^2) pasture means symbolized by sampling bout. The Ordinary Least Square (OLS) regression lines show the effect of the stocking rate (AUM per hectare) on the mean biomass by pasture for each sampling bout. The black line and black symbol refer to sampling bout one (SB1) data; the blue line and plus symbol refer to sample bout two (SB2) data; the red line and astrick refer to sampling bout three data (SB3) data.

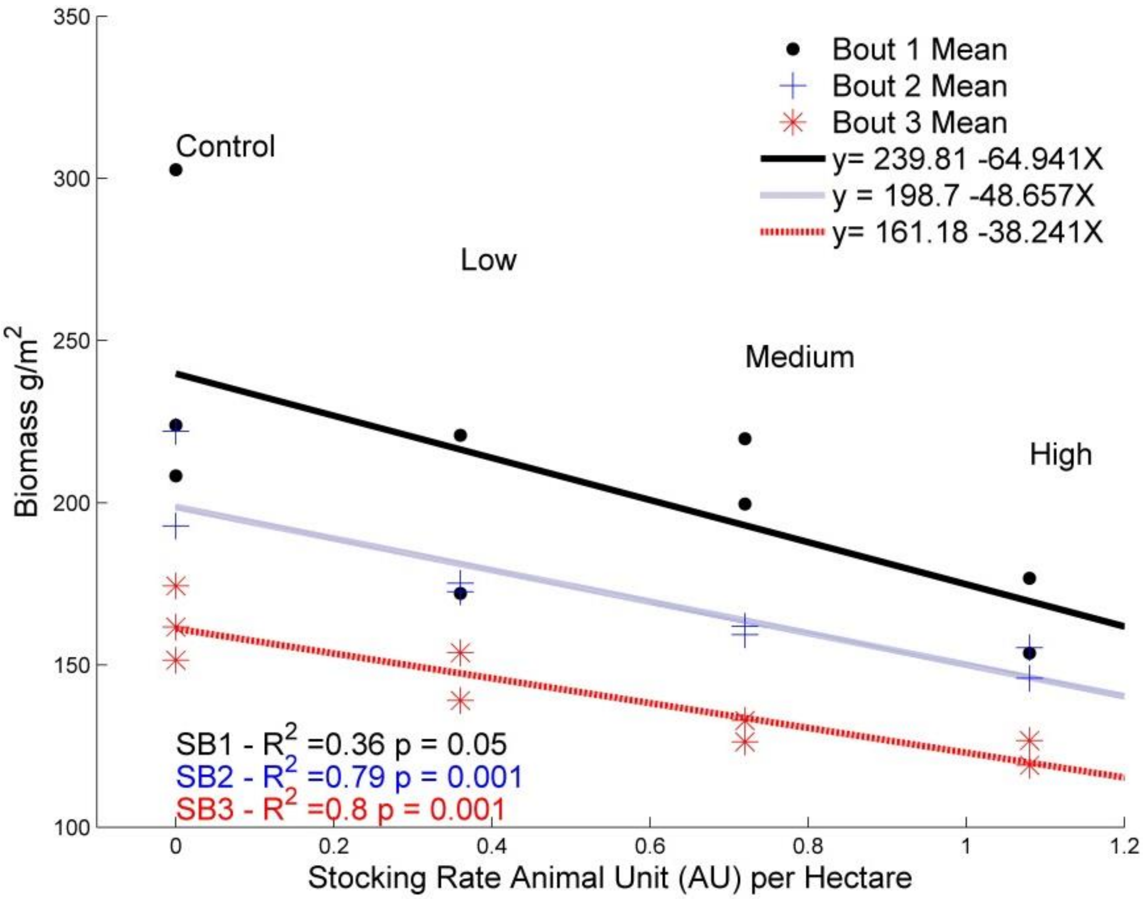

Table 1. Field metrics collected for each sampling bout across the growing season for each macro plot (N=32).

Sample bouts	Biophysical metrics	Method	Samples per site
1,2,3	Foliar cover	Line-point intercept - Herrick et al., 2005	N = 60
1,2,3	Soil surface	Line-point intercept - Herrick et al., 2005	N = 60
1,2,3	Foliar color	Line-point intercept - Herrick et al., 2005	N = 60
1,2,3	Biomass green	Clip plots	N = 4
1,2,3	Biomass brown	Clip plots	N = 4
1,2,3	Total biomass	Clip plots	N = 4
1,2,3	Vegetation structure	Robel et al. 1970	N = 13
3	Utilization	Parsons et al. 2003	N = 10

Table 2. The vegetation indices used for correlations and regressions with field metrics.

	Index and abbriviation	Formula	Reference
Red- NIR Veg. Indices	Simple Ratio (SR)	$\frac{NIR}{RED}$	Jordan (1969)
	Normalized Difference Vegetation Index (NDVI)	$\frac{NIR - RED}{NIR + RED}$	Rouse et al. (1973); Tucker (1979)
	Soil Adjusted Vegetation Index (SAVI)	$\frac{NIR-RED}{NIR+RED+0.5}(1+0.5)$	Huete (1988)
	Renormalized Difference Vegetation Index (RDVI)	$\frac{NIR - RED}{\sqrt{(NIR + RED)}}$	Ruejean and Breon (1995); Haboudane et al. (2004)
	Modified Triangular Vegetation Index 1 (MTVI1)	$1.2[1.2(NIR-GREEN)-2.5(RED-GREEN)]$	Haboudane et al. (2004)
Green/SWIR 1 Veg Indices	Plant Senesce Reflectance Index (PSRI)	$\frac{RED - GREEN}{NIR}$	Merzlyak et al. (1999)
	Canopy Index (CI)	$SWIR1- GREEN$	Vescovo & Gianelle (2008)
	Normalized Canopy Index (NCI)	$\frac{SWIR1 - GREEN}{SWIR1 + GREEN}$	Vescovo & Gianelle (2008)
	Ratio Cover Index (RCI)	$\frac{SWIR1}{RED}$	Zhang & Guo (2008)
	Normalized Difference Cover Index (NDCI)	$\frac{SWIR1 - RED}{SWIR1 + RED}$	Zhang & Guo (2008)
SWIR 2 Veg. Indices	Normalized Difference Water Index (NDWI)	$\frac{NIR - SWIR1}{NIR + SWIR1}$	Hardisky et al. (1983); Gao (1996)
	Seven/Four ratio	$\frac{SWIR2}{NIR}$	
	Normalized Difference Infrared Index 7 (NDII7)	$\frac{NIR - SWIR2}{NIR + SWIR2}$	Hardisky et al. (1983)
	Soil Adjusted Total Vegetation Index (SATVI)	$\frac{SWIR1-RED}{SWIR1+RED+0.5} * (1+0.5)\text{-}(SWIR2/2)$	Marsett et al. (2006)
Tasseled Cap	Brightness Index (BI)	$0.2043_{blue} + 0.4158_{green} + 0.5524_{red} + 0.5741_{NIR} + 0.3124_{SWIR1} + 0.2303_{SWIR2}$	Crist (1985)
	Greeness Index (GVI)	$-0.1603_{blue} - 0.2819_{green} - 0.4934_{red} + 0.7940_{NIR} - 0.0002_{SWIR1} - 0.1446_{SWIR2}$	Crist (1985)
	Wetness Index (WI)	$0.0315_{blue} + 0.2021_{green} + 0.3102_{red} + 0.1594_{NIR} - 0.6806_{SWIR1} - 0.6109_{SWIR2}$	Crist (1985)

Table 3. Pearson's correlation values between vegetation structure data and remotely sensed data, vegetation indices, and tasseled cap transformations. Values in boxes are significant at the 0.05 p value.

Remotely sensed data	Sample bout 1		Sample bout 2		Sample bout 3	
	r	p val	r	p val	r	p val
Band 1	-0.15	0.40	-0.20	0.28	0.19	0.29
Band 2	0.05	0.78	-0.16	0.38	-0.15	0.41
Band 3	-0.01	0.98	0.02	0.91	-0.02	0.91
Band 4	0.33	0.06	0.15	0.41	0.17	0.37
Band 5	-0.15	0.40	0.04	0.85	-0.15	0.41
Band 7	**-0.44**	**0.01**	**-0.53**	**0.00**	**-0.58**	**0.00**
Simple Ratio (SR)	-0.23	0.21	0.23	0.21	0.27	0.14
Normalized Difference Vegetation Index (NDVI)	0.22	0.23	-0.31	0.09	0.26	0.15
Soil Adjusted Vegetation Index (SAVI)	0.27	0.14	0.16	0.37	0.27	0.13
Renormalized Difference Vegetation Index (RDVI)	0.26	0.15	0.16	0.37	0.27	0.13
Modified Triangular Vegetation Index 1 (MTVI1)	0.24	0.18	0.14	0.45	0.21	0.26
Canopy Index (CI)	-0.21	0.24	0.10	0.59	-0.06	0.73
Normalized Canopy Index (NCI)	**-0.42**	**0.02**	0.20	0.27	0.08	0.67
Ratio Cover Index (RCI)	-0.18	0.34	0.00	1.00	-0.13	0.48
Normalized Difference Cover Index (NDCI)	-0.19	0.29	0.02	0.93	-0.12	0.50
Plant Senesce Reflectance Index (PSRI)	-0.13	0.47	0.18	0.33	0.28	0.13
Soil Adjusted Total Vegetation Index (SATVI)	0.04	0.85	0.31	0.08	0.18	0.32
Seven/Four ratio	**-0.49**	**0.00**	**-0.48**	**0.01**	**-0.54**	**0.00**
Normalized Difference Infrared Index 7 (NDII7)	**0.46**	**0.01**	**0.46**	**0.01**	**0.54**	**0.00**
Normalized Difference Water Index (NDWI)	**0.35**	**0.05**	0.18	0.32	**0.39**	**0.03**
Tasseled Cap - Brightness Index (BI)	0.10	0.59	-0.05	0.80	-0.11	0.55
Tasseled Cap - Greeness Index (GVI)	0.30	0.09	0.24	0.19	**0.37**	**0.04**
Tasseled Cap - Wetness Index (WI)	**0.39**	**0.03**	0.32	0.07	**0.47**	**0.01**

Table 4. Pearson's correlation values between percent canopy cover and remotely sensed data, vegetation indices and tasseled cap transformations. Values in boxes are significant at the 0.05 p value.

Remotely sensed data	Sample bout 1		Sample bout 2		Sample bout 3	
	r	p val	r	p val	r	p val
Band 1	0.17	0.34	-0.34	0.06	0.19	0.28
Band 2	-0.15	0.41	-0.28	0.13	0.00	1.00
Band 3	-0.25	0.17	-0.08	0.67	0.23	0.20
Band 4	**0.44**	**0.01**	0.33	0.06	**0.58**	**0.00**
Band 5	-0.31	0.09	0.00	0.99	0.25	0.17
Band 7	**-0.60**	**0.00**	**-0.66**	**0.00**	**-0.48**	**0.00**
Simple Ratio (SR)	**-0.47**	**0.01**	**0.43**	**0.01**	**0.46**	**0.01**
Normalized Difference Vegetation Index (NDVI)	**0.46**	**0.01**	**-0.48**	**0.01**	**0.46**	**0.01**
Soil Adjusted Vegetation Index (SAVI)	**0.47**	**0.01**	**0.38**	**0.03**	**0.57**	**0.00**
Renormalized Difference Vegetation Index (RDVI)	**0.47**	**0.01**	**0.38**	**0.03**	**0.57**	**0.00**
Modified Triangular Vegetation Index 1 (MTVI1)	**0.43**	**0.01**	**0.36**	**0.04**	**0.51**	**0.00**
Canopy Index (CI)	-0.34	0.05	0.10	0.58	0.31	0.08
Normalized Canopy Index (NCI)	**-0.35**	**0.05**	0.29	0.11	0.18	0.33
Ratio Cover Index (RCI)	0.13	0.49	0.11	0.55	-0.10	0.60
Normalized Difference Cover Index (NDCI)	0.11	0.55	0.11	0.56	-0.08	0.67
Plant Senesce Reflectance Index (PSRI)	**-0.37**	**0.04**	-0.05	0.77	0.23	0.20
Soil Adjusted Total Vegetation Index (SATVI)	0.27	0.14	**0.42**	**0.02**	0.33	0.06
Seven/Four ratio	**-0.66**	**0.00**	**-0.68**	**0.00**	**-0.75**	**0.00**
Normalized Difference Infrared Index 7 (NDII7)	**0.63**	**0.00**	**0.66**	**0.00**	**0.74**	**0.00**
Normalized Difference Water Index (NDWI)	**0.53**	**0.00**	**0.45**	**0.01**	**0.55**	**0.00**
Tasseled Cap - Brightness Index (BI)	-0.02	0.91	-0.04	0.84	0.24	0.18
Tasseled Cap - Greeness Index (GVI)	**0.49**	**0.00**	**0.46**	**0.01**	**0.67**	**0.00**
Tasseled Cap - Wetness Index (WI)	**0.54**	**0.00**	**0.43**	**0.01**	0.24	0.18

Table 5. Pearson's correlation values between dry biomass data and remotely sensed data, vegetation indices and tasseled cap transformations. Values in boxes are significant at the 0.05 p value.

Remotely sensed data	Sample bout 1		Sample bout 2		Sample bout 3	
	r	p val	r	p val	r	p val
Band 1	-0.07	0.72	-0.27	0.14	0.23	0.20
Band 2	0.04	0.83	-0.19	0.29	-0.11	0.55
Band 3	-0.02	0.93	-0.02	0.92	0.09	0.61
Band 4	**0.40**	**0.02**	**0.46**	**0.01**	**0.43**	**0.01**
Band 5	-0.12	0.50	0.22	0.22	0.08	0.65
Band 7	**-0.43**	**0.01**	**-0.48**	**0.01**	**-0.41**	**0.02**
Simple Ratio (SR)	-0.27	0.14	**0.51**	**0.00**	**0.45**	**0.01**
Normalized Difference Vegetation Index (NDVI)	0.26	0.15	**-0.54**	**0.00**	**0.44**	**0.01**
Soil Adjusted Vegetation Index (SAVI)	0.33	0.07	**0.48**	**0.01**	**0.51**	**0.00**
Renormalized Difference Vegetation Index (RDVI)	0.31	0.08	**0.48**	**0.01**	**0.51**	**0.00**
Modified Triangular Vegetation Index 1 (MTVI1)	0.30	0.10	**0.47**	**0.01**	**0.46**	**0.01**
Canopy Index (CI)	-0.17	0.35	0.32	0.07	0.15	0.40
Normalized Canopy Index (NCI)	-0.34	0.06	**0.41**	**0.02**	0.20	0.28
Ratio Cover Index (RCI)	-0.11	0.55	0.31	0.08	-0.07	0.71
Normalized Difference Cover Index (NDCI)	-0.13	0.46	0.32	0.08	-0.05	0.78
Plant Senesce Reflectance Index (PSRI)	-0.14	0.43	-0.22	0.23	0.23	0.21
Soil Adjusted Total Vegetation Index (SATVI)	0.13	0.48	**0.58**	**0.00**	0.23	0.20
Seven/Four ratio	**-0.52**	**0.00**	**-0.66**	**0.00**	**-0.57**	**0.00**
Normalized Difference Infrared Index 7 (NDII7)	**0.49**	**0.00**	**0.65**	**0.00**	**0.58**	**0.00**
Normalized Difference Water Index (NDWI)	**0.39**	**0.03**	**0.44**	**0.01**	**0.50**	**0.00**
Tasseled Cap - Brightness Index (BI)	0.14	0.43	0.16	0.39	0.11	0.56
Tasseled Cap - Greeness Index (GVI)	**0.37**	**0.04**	**0.52**	**0.00**	**0.57**	**0.00**
Tasseled Cap - Wetness Index (WI)	**0.38**	**0.03**	0.19	0.30	0.26	0.15

Table 6. Vertical structure regression models. Models of full, step-wise and best subset models for up to 4 predictor variables are shown. The “best” model selected is bolded and was chosen based on the lowest corrected AIC and an acceptable variance inflation factor (<10).

	Selected variables	Intercept	B1	B2	B3	B4	B5	B7	SR	NDVI	SAVI	RDVI	MTVII	CI	NCI	RCI	NDCI	PSRI	SATVI	SF	NBR	NDWI	TCBI	TCGVI	TCWI	Total Paramters	R2	Adj. R2	Residual SE	AIC	AICc	p-value	parameter with a VIF value over 10
Sample Bout -1																																	
Full	23	NS	NS	NS	NS	NS	NS	NS	NS	NS	NS	NS	NS	NS	NS	NS	NS	NS	NS	NS	NS	NS	NS	NS	NS	24	0.844	0.63	0.25	13.98	185.41	0.01	Yes
Stepwise	12	0.1	NS				0.1		0.1	0.05		0.05					0.05		0.05	0.05						13	0.817	0.70	0.23	7.01	31.72	9.69E-05	Yes
Best Subset	1	0.001																		0.01						2	0.242	0.22	0.37	30.57	30.98	4.28E-03	No
Best Subset	2	0.001			0.001			0.001																		3	0.699	0.68	0.24	3.05	3.91	2.82E-08	No
Best Subset	**3**	**0.001**	**0.001**									**0.001**								**0.001**						**4**	**0.732**	**0.70**	**0.23**	**1.29**	**2.77**	**4.15E-06**	**No**
Best Subset	4	0.01	NS						0.01												0.001			0.05		5	0.747	0.71	0.22	1.38	3.69	9.49E-08	Yes
Sample Bout - 2 - Outliers removed N = 30																																	
Full	23	NS	NS	NS	NS	NS	NS	NS	NS	NS	NS	NS	NS	NS	NS	NS	NS	NS	NS	NS	NS	NS	NS	NS	NS	24	0.755	0.35	0.20	-2.99	237.01	1.42E-01	Yes
Stepwise	13	0.05			NS	NS	0.1	0.1		NS	NS	NS				0.1	0.1		0.1		0.1	0.1				14	0.745	0.57	0.16	-13.76	14.24	4.03E-03	Yes
Best Subset	1	0.001						0.01																		2	0.266	0.24	0.21	-2.27	-1.83	7.03E-03	No
Best Subset	**2**	**0.001**																		**0.001**		**0.001**				**3**	**0.517**	**0.48**	**0.18**	**-14.58**	**-13.66**	**5.44E-05**	**No**
Best Subset	3	NS										0.001					0.01				0.001					4	0.592	0.55	0.16	-17.67	-16.07	2.85E-05	Yes
Best Subset	4	NS					0.01				0.01	0.01									0.001					5	0.624	0.56	0.16	-18.11	-15.61	4.31E-05	Yes
Sampling Bout - 3																																	
Full	23	NS	NS	NS	NS	NS	0.1	0.05	NS	NS	NS	NS	NS	NS	0.1	NS	NS	0.05	NS	NS	NS	NS	NS	NS	0.1	24	0.660	0.19	0.27	17.10	217.10	0.2654	Yes
Stepwise	10	0.05							0.1	0.1		NS				NS		0.05		NS	NS	0.05				11	0.631	0.46	0.22	-3.67	17.57	6.47E-03	Yes
Best Subset	1	0.001						0.001																		2	0.328	0.30	0.22	-2.38	-1.95	7.63E-04	No
Best Subset	**2**	**0.05**					**NS**	**0.001**																		**3**	**0.389**	**0.35**	**0.24**	**3.82**	**4.71**	**7.83E-04**	**No**
Best Subset	3	NS														0.05					0.001			0.01		4	0.453	0.39	0.23	2.28	3.82	6.46E-04	Yes
Best Subset	4	0.01				0.05													0.05		0.01				0.05	5	0.488	0.41	0.23	2.21	4.61	9.10E-04	Yes

Table 7. Cover regression models. Models of full, step-wise and best subset models for up to 4 predictor variables are shown. The “best” model selected is bolded and was chosen based on the lowest corrected AIC and an acceptable variance inflation factor (<10).

Sample Bout - 1	Selected variables	Intercept	B1	B2	B3	B4	B5	B7	SR	NDVI	SAVI	RDVI	MTVII	CI	NCI	RCI	NDCI	PSRI	SATVI	SF	NBR	NDWI	TCBI	TCGVI	TCWI	Total Parameters	R2	Adj. R2	Residual SE	AIC	AICc	p-value	parameter with a VIF value over 10
Full	23	NS	NS	NS	NS	NS	NS	NS	NS	NS	NS	NS	NS	NS	NS	NS	NS	NS	NS	NS	NS	NS	NS	NS	NS	24	0.820	0.57	0.12	-33.15	138.27	0.02	Yes
Stepwise	13	0.05		0.1	0.1	0.1	0.1			0.1	0.1	0.1				0.1		0.1		NS	0.1	0.1				14	0.809	0.69	0.10	-43.16	-22.94	1.41E-04	Yes
Best Subset	1	0.001																		0.001						2	0.441	0.42	0.14	-30.77	-30.36	3.43E-05	No
Best Subset	2	0.001																		0.001				0.001		3	0.651	0.63	0.11	-43.91	-43.06	2.30E-07	No
Best Subset	**3**	**0.001**					**0.1**						**0.001**							**0.001**						**4**	**0.703**	**0.67**	**0.11**	**-47.05**	**-45.57**	**1.51E-07**	**No**
Best Subset	4	0.001								0.1	0.05	0.05								0.05						5	0.724	0.68	0.10	-47.40	-45.09	3.01E-07	Yes
Sample Bout - 2																																	
Full	23	NS	NS	NS	NS	NS	NS	NS	NS	NS	NS	NS	NS	NS	NS	NS	NS	NS	NS	NS	NS	NS	NS	NS	NS	24	0.830	0.60	0.10	-44.80	155.20	1.25E-02	Yes
Stepwise	10	NS	0.1		0	0		NS	0			0.01							0.05		0.1	0				11	0.811	0.72	0.08	-57.38	-31.13	1.39E-05	Yes
Best Subset	1	0.001																		0.001						2	0.467	0.45	0.12	-46.41	-41.80	1.62E-05	No
Best Subset	**2**	**0.001**									**0.001**									**0.001**						**3**	**0.642**	**0.62**	**0.10**	**-52.97**	**-52.11**	**3.35E-07**	**No**
Best Subset	3	0.001										0.01				NS				0.001						4	0.672	0.64	0.10	-53.72	-52.18	6.06E-07	Yes
Best Subset	4	0.01											0.001			0.05	0.1			0.05						5	0.715	0.67	0.09	-56.18	-53.87	4.76E-07	Yes
Sample Bout - 3																																	
Full	23	NS	0.1	NS	NS	NS	NS	NS	NS	NS	NS	NS	NS	NS	NS	NS	NS	NS	NS	NS	NS	NS	NS	NS	NS	24	0.811	0.55	0.11	-41.60	129.83	2.15E-02	Yes
Stepwise	14	NS	0.1	NS	NS		0.1	0.1		NS	NS	NS				NS		NS	0.05			0.1				15	0.802	0.64	0.09	-48.14	-18.14	1.27E-03	Yes
Best Subset	1	0.001																		0.001						2	0.560	0.55	0.11	-48.54	-48.13	8.54E-07	No
Best Subset	**2**	**0.001**														**0.001**			**0.001**							**3**	**0.665**	**0.64**	**0.09**	**-55.42**	**-54.57**	**1.22E-07**	**No**
Best Subset	3	0.05		NS												0.001			0.001							4	0.67	0.64	0.09	-54.18	-52.70	5.48E-07	No
Best Subset	4	0.05	0.1	0.1												0.001			0.001							5	0.706	0.66	0.09	-55.41	-53.11	7.12E-07	Yes

Table 8. Biomass regression models. Models of full, step-wise and best subset models for up to 4 predictor variables are shown. The “best” model selected is bolded and was chosen based on the lowest corrected AIC and an acceptable variance inflation factor (<10).

	Selected variables	Intercept	B1	B2	B3	B4	B5	B7	SR	NDVI	SAVI	RDVI	MTVII	CI	NCI	RCI	NDCI	PSRI	SATVI	SF	NBR	NDWI	TCBI	TCGVI	TCWI	Total Paramters	R2	Adj. R2	Residual SE	AIC	AICc	p-value	parameter with a VIF value over 10
Sample Bout - 1																																	
Full	23	NS	NS	NS	0.05	0.05	NS	NS	0.1	0.01	0.01	0.05	NA	NA	0.001	0.05	NS	0.01	NS	NS	0.05	0.01	NA	NA	NA	24	0.895	0.75	44.46	344.85	516.27	1.90E-03	Yes
Stepwise	14	NS			0.01	0.01	0.01	0.01	0.05	0.01	0.01	0.01			0.001	0.01		0.001		0.01	0.01	0.01				15	0.883	0.79	41.09	340.38	365.08	2.44E-05	Yes
Best Subset	1	0.001																		0.01						2	0.269	0.24	77.27	372.98	373.39	2.54E-03	No
Best Subset	**2**	**0.001**																**0.001**		**0.001**						**3**	**0.674**	**0.65**	**52.49**	**349.14**	**349.99**	**8.75E-08**	**No**
Best Subset	3	0.05								NS								NS		0.001						4	0.683	0.65	52.68	350.25	351.73	3.78E-07	Yes
Best Subset	4	0.001				0.1					0.05	0.05								0.001						5	0.716	0.67	50.74	348.69	350.99	4.38E-07	Yes
Sample Bout - 2																																	
Full	23	NS	NS	NS	0.1	0.1	NS	NS	0.05	0.1	0.1	0.1	NA	NA	NS	NS	0.1	NS	NS	NS	0.05	0.05	NA	NA	NA	24	0.854	0.65	43.75	343.81	515.24	5.71E-03	Yes
Stepwise	16	0.05	NS	NS	0.01	0.01	0.05	0.05	0.05	0.01	0.01	0.01				0.05	0.05	NS		NS	0.01	0.05				17	0.850	0.69	41.20	340.55	384.27	1.16E-03	Yes
Best Subset	1	0.001																		0.001						2	0.438	0.42	56.42	352.84	353.26	3.70E-05	No
Best Subset	**2**	**0.001**																		**0.001**		**0.01**				**3**	**0.569**	**0.54**	**50.26**	**346.37**	**347.22**	**5.04E-06**	**No**
Best Subset	3	NS																	0.01		0.001			0.01		4	0.595	0.55	49.57	346.37	347.83	1.09E-05	Yes
Best Subset	4	0.05								0.01				0.01							0.001			0.01		5	0.652	0.60	46.82	343.54	345.84	6.41E-06	No
Sample Bout 3 - Outliers Removed - N = 31																																	
Full	23	NS	NS	NS	NS	NS	0.05	0.05	NS	NS	NS	NS	NA	NA	NS	NS	NS	NS	0.05	0.01	NS	NS	NA	NA	NA	24	0.827	0.57	39.86	327.04	527.04	2.27E-02	Yes
Stepwise	14	0.1		NS	0.001	0.001	0.001	0.001	0.001	0.001		0.001					0.001	NS	0.001	0.001		0.1				15	0.813	0.67	34.83	319.48	351.48	6.07E-04	Yes
Best Subset	**1**	**0.001**																			**0.001**					**2**	**0.346**	**0.32**	**49.86**	**334.28**	**334.71**	**5.04E-04**	**No**
Best Subset	2	NS																		NS	NS					3	0.350	0.30	50.57	336.07	336.96	2.40E-03	Yes
Best Subset	3	NS				NS		NS												NS						4	0.371	0.30	50.65	337.04	338.58	5.20E-03	Yes
Best Subset	4	0.1						NS		NS	NS									NS						5	0.367	0.27	51.79	339.27	341.65	1.51E-02	Yes

Bibliography

Akaike, H. (1974). A new look at the statistical model identification. *Automatic Control, IEEE Transactions on*, *AC-19*(6), 716–723.

Allen-Diaz, B., Chapin, F. S., Diaz, S., M. Howden, J. P., & Smith, M. S. (1995). Rangelands in a Changing Climate: Impacts, Adaptations, and Mitigation. *In: Climate Change 1995—Impacts, Adaptation and Mitigation, W. T. Watson, M. C. Zinyowera, R. H. Moss, and D. J. Dokken, (eds.), Pg. 131–158*.

Anderson, G. L., Hanson, J. D., & Haas, R. H. (1993). Evaluating Landsat Thematic Mapper Derived Vegetation Indices for Estimating Above-Ground Biomass on Semiarid Ranglelands. *Remote Sensing Environment*, *45*, 165–175.

Archer, E. R. M. (2004). Beyond the "' climate versus grazing '" impasse : using remote sensing to investigate the effects of grazing system choice on vegetation cover in the eastern Karoo. *Journal of Arid Environments*, *57*, 381–408. doi:10.1016/S0140-1963(03)00107-1

Bartuszevige, A. M., Kennedy, P. L., & Taylor, R. V. (2012). Sixty-seven Years of Landscape Change in the Last, Large Remnant of the Pacific Northwest Bunchgrass Prairie. *Natural Areas Journal*, *32*(2), 166–170.

Bastin, G., Scarth, P., Chewings, V., Sparrow, A., Denham, R., Schmidt, M., O'Reagain, P., Shepherd, R., Abbott, B. (2012). Separating grazing and rainfall effects at regional scale using remote sensing imagery: A dynamic reference-cover method. *Remote Sensing of Environment*, *121*, 443–457. doi:10.1016/j.rse.2012.02.021

Blanco, L. J., Ferrando, C. A., & Biurrun, F. N. (2009). Remote Sensing of Spatial and Temporal Vegetation Patterns in Two Grazing Systems. *Rangeland Ecology and Management*, *62*(5), 445–451.

Booth, D. T., & Tueller, P. T. (2003). Rangeland monitoring using remote sensing. *Arid Land Research and Management*, *17*, 455–467.

Bradley, B. A., & O'sullivan, M. T. (2011). Assessing the short-term impacts of changing grazing regime at the landscape scale with remote sensing. *International Journal of Remote Sensing*, *32*(20), 5797–5813.

Brinkmann, K., Dickhoefer, U., Schlecht, E., & Buerkert, A. (2011). Quantification of aboveground rangeland productivity and anthropogenic degradation on the Arabian Peninsula using Landsat imagery and field inventory data. *Remote Sensing of Environment*, *115*(2), 465–474. doi:10.1016/j.rse.2010.09.016

Butterfield, H. S., & Malmstrom, C. M. (2006). Experimental Use of Remote Sensing by Private Range Managers and Its Influence on Management Decisions. *Rangeland Ecology and Management*, *59*(5), 541–548.

Chander, G., Markham, B. L., & Helder, D. L. (2009). Summary of current radiometric calibration coefficients for Landsat MSS, TM, ETM+, and EO-1 ALI sensors. *Remote Sensing of Environment*, *113*(5), 893–903. doi:10.1016/j.rse.2009.01.007

Chavez, P. (1996). Image-based atmospheric corrections-revisited and improved. *Photogrammetric Engineering and Remote Sensing*, *62*(9), 1025–1036.

Cliff, A. ., & Ord, J. K. (1981). *Spatial Processes, Models and Applications.* (pp. 19–22). London: Pion.

Conner, R., Seidl, A., VanTassell, L., & Wilkins, N. (2002). United States Grasslands and Related Resources: An Economic and Biological Trends Assessment. *The National Cattlemen's Beef Association, The Nature Conservancy and Ducks Unlimited*.

Coulloudon, B., Eshelman, K., Gianola, J., Habich, N., Hughes, L., Johnson, C., Pellant, M., Podborny, P., Rasmussen, A., Robles, B., Shaver, P., Spehar, J., Willoughby, J. (1999). Sampling Vegetation Attributes. Interagency Technical Reference, 171.

Crist, E., & Kauth, R. (1986). The tasseled cap de-mystified. *Photogrammetric Engineering and Remote Sensing*, *52*(1), 81–86.

Dungan, J. (1998). Spatial prediction of vegetation quantities using ground and image data. *International Journal of Remote Sensing*, *19*(2), 267–285. doi:10.1080/014311698216242

Evans, J., & Geerken, R. (2004). Discrimination between climate and human-induced dryland degradation. *Journal of Arid Environments*, *57*(4), 535–554. doi:10.1016/S0140-1963(03)00121-6

Friendly, M., & Kwan, E. (2009). Where's Waldo? Visualizing Collinearity Diagnostics. *The American Statistician*, *63*(1), 56–65. doi:10.1198/tast.2009.0012

Gao, B. (1996). NDWI A Normalized Difference Water Index for Remote Sensing of Vegetation Liquid Water From Space. *Remote Sensing of Environment*, *266*(April 1995), 257–266.

Haboudane, D. (2004). Hyperspectral vegetation indices and novel algorithms for predicting green LAI of crop canopies: Modeling and validation in the context of precision agriculture. *Remote Sensing of Environment*, *90*(3), 337–352. doi:10.1016/j.rse.2003.12.013

Hagen, S. C., Heilman, P., Marsett, R., Torbick, N., Salas, W., van Ravensway, J., & Qi, J. (2012). Mapping Total Vegetation Cover Across Western Rangelands With Moderate-Resolution Imaging Spectroradiometer Data. *Rangeland Ecology and Management*, *65*(5), 456–467. doi:10.2111/REM-D-11-00188.1

Hardisky, M. A., Smart, R. M., & Klemas, V. (1983). Seasonal Spectral Characteristics and Aboveground Biomass of the Tidal Marsh Plant, Spartina alterniflora. *American Society of Photogrammetry*, *49*(1), 85–92.

Herrick, J. E., Lessard, V. C., Spaeth, K. E., Shaver, P. L., Dayton, R. S., Pyke, D. A, Jolley, L., Goebel, J. J. (2010). National ecosystem assessments supported by scientific and local knowledge. *Frontiers in Ecology and the Environment*, *8*(8), 403–408. doi:10.1890/100017

Herrick, J. E., Zee, J. W. Van, Havstad, K. M., Burkett, L. M., Whitford, W. G., Pyke, D. A., Remmenga, M. D., Shaver, P. L. (2005). Monitoring Manual for grassland, shrubland and savanna ecosystems. Las Cruces, NM, USA: USDA-ARS Jornada Experimental Range., 236.

Hill, J., Hostert, P., Tsiourlis, G., Kasapidis, P., Udelhoven, T., & Diemer, C. (1998). Monitoring 20 years of increased grazing impact on the Greek island of Crete with earth observation satellites. *Journal of Arid Environments*, *39*(2), 165–178. doi:10.1006/jare.1998.0392

Hoekstra, J. M., Boucher, T. M., Ricketts, T. H., & Roberts, C. (2004). Confronting a biome crisis: global disparities of habitat loss and protection. *Ecology Letters*, *8*(1), 23–29. doi:10.1111/j.1461-0248.2004.00686.x

Holechek, J. (1988). An approach for setting the stocking rate. *Rangelands*, *10*(1), 10–14.

Holechek, J., & Gomez, H. (1999). Grazing studies: what we've learned. *Society of Range Management*, *21*(2), 12–16.

Hudak, A. T., Crookston, N. L., Evans, J. S., Falkowski, M. J., Smith, A. M. S., Gessler, P. E., & Morgan, P. (2006). Regression modeling and mapping of coniferous forest basal area and tree density from discrete-return lidar and multispectral satellite data. *Canadian Journal of Remote Sensing*, *32*(2), 126–138. doi:10.5589/m06-007

Huete, A. R. (1988). A soil-adjusted vegetation index (SAVI). *Remote Sensing of Environment*, *25*(3), 295–309. doi:10.1016/0034-4257(88)90106-X

Hunt, E. R., Everitt, J. H., Ritchie, J. C., Moran, M. S., Booth, D. T., Anderson, G. L., … Seyfried, M. S. (2003). Applications and Research Using Remote Sensing for Rangeland Management. *Photogrammetric Engineering and Remote Sensing*, *69*(6), 675–693.

Ikeda, H., Okamoto, K., & Fukuhara, M. (1999). Estimation of aboveground grassland phytomass with a growth model using Landsat TM and climate data. *International Journal of Remote Sensing*, *20*(11), 2283–2294.

Johnson, T. N., Kennedy, P. L., DelCurto, T., & Taylor, R. V. (2011). Bird community responses to cattle stocking rates in a Pacific Northwest bunchgrass prairie. *Agriculture, Ecosystems and Environment*, *144*(1), 338–346. doi:10.1016/j.agee.2011.10.003

Johnson, T. N., Kennedy, P. L., & Etterson, M. A. (2012). Nest success and cause-specific nest failure of grassland passerines breeding in prairie grazed by livestock. *The Journal of Wildlife Management*, *76*(8), 1607–1616. doi:10.1002/jwmg.437

Jordan, C. (1969). Derivation of leaf-area index from quality of light on the forest floor. *Ecology*, *50*(4), 663–666.

Kauth, R. J., & Thomas, G. S. (1976). The Tasselled Cap--A Graphic Description of the Spectral-Temporal Development of Agricultural Crops as Seen by LANDSAT. *LARS Symposia*.

Kawamura, K., Akiyama, T., Yokota, H., Tsutsumi, M., Yasuda, T., Watanabe, O., & Wang, S. (2005). Quantifying grazing intensities using geographic information systems and satellite remote sensing in the Xilingol steppe region, Inner Mongolia, China. *Agriculture, Ecosystems and Environment*, *107*(1), 83–93. doi:10.1016/j.agee.2004.09.008

Key, C. (2006). Ecological and sampling constraints on defining landscape fire severity. *Fire Ecology*, *2*(2), 34–59.

Key, C. H., & Benson, N. C. (2006). *Landscape Assessment (LA) Sampling and Analysis Methods* (pp. 1–55).

Kimoto, C., Debano, S. J., Thorp, R. W., Rao, S., Stephen, W. P., & William, P. (2012). Investigating Temporal Patterns of a Native Bee Community in a Remnant North American Bunchgrass Prairie using Blue Vane Traps. *Journal of Insect Science*, 12(108), 1–23.

Knipling, E. (1970). Physical and physiological basis for the reflectance of visible and near-infrared radiation from vegetation. *Remote Sensing of Environment*, *1*(3), 155–159.

Lilliefors, H. (1967). On the Kolmogorov-Smirnov test for normality with mean and variance unknown. *Journal of the American Statistical Association*, *62*(318), 399–402.

Lind, M., & Rasmussen, K. (2003). Estimating vegetative productivity gradients around watering points in the rangelands of Northern Senegal based on NOAA AVHRR data. *Danish Journal of Geography*, *103*(1), 1–16.

Marsett, R. C., Qi, J., Heilman, P., Biedenbender, S. H., Watson, M. C., Amer, S., Weltz, M., Goodrich, D., Marsett, R. (2006). Remote Sensing for Grassland Management in the Arid Southwest. *Rangeland Ecology and Management*, 59(5), 530–540.

McLean, A., & Tisdale, E. (1972). Recovery rate of depleted range sites under protection from grazing. *Journal of Range Management*, 178–184.

Merzlyak, M. N., Gitelson, A. A., Chivkunova, O. B., & Rakitin, Y. (1999). Non-destructive optical detection of pigment changes during leaf senescence and fruit ripening. *Physiologia Plantarum*, *106*, 135–141.

Milchunas, D., & Lauenroth, W. (1993). Quantitative effects of grazing on vegetation and soils over a global range of environments. *Ecological Monographs*, *63*(4), 327–366.

Munyati, C., & Makgale, D. (2009). Multitemporal Landsat TM imagery analysis for mapping and quantifying degraded rangeland in the Bahurutshe communal grazing lands, South Africa. *International Journal of Remote Sensing*, *30*(14), 3649–3668. doi:10.1080/01431160802592534

Numata, I., Roberts, D. A., Chadwick, O. A., Schimel, J., Sampaio, F. R., Leonidas, F. C., & Soares, J. V. (2007). Characterization of pasture biophysical properties and the impact of grazing intensity using remotely sensed data. *Remote Sensing of Environment*, *109*(3), 314–327. doi:10.1016/j.rse.2007.01.013

Parsons, C. T., Momont, P. A., Delcurto, T., Mcinnis, M., Porath, L., & Marni, L. (2003). Cattle distribution patterns and vegetation use in mountain riparian areas. *Journal Of Range Management*, *56*(4), 334–341.

Paudel, K. P., & Andersen, P. (2010). Assessing rangeland degradation using multi temporal satellite images and grazing pressure surface model in Upper Mustang, Trans Himalaya, Nepal. *Remote Sensing of Environment*, *114*(8), 1845–1855. doi:10.1016/j.rse.2010.03.011

Pickup, G., Bastin, G. N., & Chewings, V. H. (1994). Remote-Sensing-Based Condition Assessment for Nonequilibrium Rangelands Under Large- Scale Commercial Grazing. *Ecological Society of America*, *4*(3), 497–517.

Pickup, G., Bastin, G. N., & Chewings, V. H. (1998). Identifying trends in land degradation in non-equilibrium rangelands. *Journal of Applied Ecology*, *35*(3), 365–377. doi:10.1046/j.1365-2664.1998.00319.x

Purevdorj, T., & Tateishi, R. (1998). Relationships between percent vegetation cover and vegetation indices. *International Journal of Remote Sensing*, *19*(18), 3–18.

Robel, R. I., Briggs, J. N., Dayton, A. D., & Hulbert, L. C. (1970). Relationships between Visual Obstruction Measurements and Weight of Grassland Vegetation Relationships Between Visual Obstruction Measurements and Weight of Grassland Vegetation. *Journal Of Range Management*, *23*(4), 295–297.

Roberts, D. A., Smith, M. O., & Adams, J. B. (1993). Green vegetation, nonphotosynthetic vegetation, and soils in AVIRIS data. *Remote Sensing of Environment*, *44*(2-3), 255–269. doi:10.1016/0034-4257(93)90020-X

Röder, A., Udelhoven, T., Hill, J., del Barrio, G., & Tsiourlis, G. (2008). Trend analysis of Landsat-TM and -ETM+ imagery to monitor grazing impact in a rangeland ecosystem in Northern Greece. *Remote Sensing of Environment*, *112*(6), 2863–2875. doi:10.1016/j.rse.2008.01.018

Roujean, J., & Breon, F. (1995). Estimating PAR absorbed by vegetation from bidirectional reflectance measurements. *Remote Sensing of Environment*, *51*(3), 375–384.

Rouse, W., Haas, H., & Deering, W. (1973). 20 monitoring vegetation systems in the great plains with erts . *Proceeding of 3rd ERTS Symposium*.

Schino, G., Borfecchia, F., & Cecco, L. De. (2003). Satellite estimate of grass biomass in a mountainous range in central Italy. *Agroforestry Systems*, *59*, 157–162.

Skovlin, J. M., Harris, R. W., Strickler, G. S., & Garrison, G. A. (1976). *Effects of cattle grazing methods on ponderosa pine-bunchgrass range in the Pacific Northwest* (p. 48).

Sugiura, N. (1978). Further analysts of the data by Akaike's information criterion and the finite corrections. *Communications in Statistics - Theory and Methods*, *A7*(No. 1), pp. 13–26.

Todd, S., Hoffer, R., & Milchunas, D. (1998). Biomass estimation on grazed and ungrazed rangelands using spectral indices. *International Journal of Remote Sensing*, *19*(3), 427–438.

Tucker, C. (1980). Remote sensing of leaf water content in the near infrared. *Remote Sensing of Environment*, *10*(1), 23–32.

Tucker, C. J. (1979). Red and photographic infrared linear combinations for monitoring vegetation. *Remote Sensing of Environment*, *8*, 127–150.

Vescovo, L., & Gianelle, D. (2008). Using the MIR bands in vegetation indices for the estimation of grassland biophysical parameters from satellite remote sensing in the Alps region of Trentino (Italy). *Advances in Space Research*, *41*(11), 1764–1772. doi:10.1016/j.asr.2007.07.043

Washington-Allen, R. A., West, N. E., Ramsey, R. D., & Efroymson, R. A. (2006). A Protocol for Retrospective Remote Sensing – Based Ecological Monitoring of Rangelands Special l Monitoring of Rangelands. *Rangeland Ecology and Management*, *59*(1), 19–29.

West, N. E. (2003). History of Rangeland Monitoring in the U . S . A . *Arid Land Research and Management*, *17*(4), 495–545. doi:10.1080/15324980390225584

Wulder, M. A., White, J. C., Masek, J. G., Dwyer, J., & Roy, D. P. (2011). Continuity of Landsat observations: Short term considerations. *Remote Sensing of Environment*, *115*(2), 747–751. doi:10.1016/j.rse.2010.11.002

Wylie, B., Meyer, D., Tieszen, L., & Mannel, S. (2002). Satellite mapping of surface biophysical parameters at the biome scale over the North American grasslands: a case study. *Remote Sensing of Environment*, *79*, 266–278.

Yang, X., & Guo, X. (2011). Investigating vegetation biophysical and spectral parameters for detecting light to moderate grazing effects: a case study in mixed grass prairie. *Central European Journal of Geosciences*, *3*(3), 336–348. doi:10.2478/s13533-011-0032-4

Zhang, C., & Guo, X. (2008). Monitoring northern mixed prairie health using broadband satellite imagery. *International Journal of Remote Sensing*, *29*(8), 2257–2271. doi:10.1080/01431160701408378

Chapter 2: Applications to Management

The ability of remote sensing to gather data across large spatial extents has the potential to provide unwitting and sometimes undesirable dissemination of private information, but it also has the potential to democratize data collection, increase societal awareness of important issues, and enhance transparency of actions (Myers, 2010). Therefore successful application and dissemination of remotely sensed data and analysis products to the rangeland community provided by this research will rely on both social and scientific knowledge. Recent research has shown that remotely sensed data can provide monitoring information that agrees with rancher's perception of grassland productivity (Rowley et al., 2007) as well as provide private land owners a tool to assess and inform management action (Butterfield and Malmstrom, 2006). Balancing the potential of easily accessed and shared remotely sensed data with the various desires of landowners to keep data private will be an important step in collaborating and implementing the use of remotely sensed data products to better manage lands across the Zumwalt Prairie.

In previous work conducted by Butterfield and Malmstrom. (2006) remotely sensed data products were only made available to the owners of each land parcel analyzed. While some ranchers kept their data private, it was also observed that two of the cattle ranchers shared their data, improving the decision making and management action across ownership boundaries (Butterfield and Malmstrom, 2006). It is foreseeable that some individual or groups ranchers on the Zumwalt Prairie would agree to share data across ownership to better understand what is happening across their private lands due to trans-boundary forces, such as heavy elk use. This ability to share data across various temporal and spatial scales that is consistently collected and common among landowners highlights the potential of remote sensed data to provide meaningful information which can be easily discussed and compared within the ranching community.

As end users of remotely sensed data ranchers and land managers need to be able to interact with the data in a straightforward way, and have it provide the needed information to answer their questions (Butterfield and Malmstrom, 2006). One question that is frequently asked is: what is the proper stocking rate for this land for any given year? Stocking at a rate appropriate to the amount of forage available, employing methods such as herding and salting to facilitate proper distribution and to avoid overuse of sensitive areas, as well as managing timing (both duration and rotation) are essential in avoiding negative short and long-term impacts (Holechek and Gomez, 1999; Ortega-S et al., 2013). It is our goal that by quantifying common rangeland metrics across a grazing season and providing spatially explicit maps and data, land managers are better equipped to understand the effects of their stocking rate and make more informed decisions going forward (Chapter 1). Marsett et al. (2006) points out that maps derived from remote sensing that quantify vegetation can then be analyzed at different scales with Geographical Information System (GIS) tools. In our study we computed the mean vegetation amounts by stocking rate treatment and pasture area, but these metrics could also be calculated at a spatial or temporal scale that best fits a ranchers needs providing retrospective measures of grazing. Quantitative grazing outcomes (e.g., measures of residual biomass, utilization, stubble height) allow land managers to evaluate whether past grazing produced intended outcomes (Coulloudon et al., 1999) and can compare these outcomes over time.

While we have demonstrated the ability for Landsat ETM+ data to model vegetation amounts and provide comparisons between stocking rates across a grazing season, the research and deployment of usable rangeland data can be improved in multiple ways. First, a better understanding of the potential productivity across the landscape would improve our understanding of grazing effects. Second, performing a multiyear time series analysis to understand the inter-annual variability of vegetation amounts as well as analyze how precipitation influences vegetation amount and greenness would improve a rancher's ability to forecast how much forage maybe available. Third, decreasing processing time by creating geoprocessing scripts that efficiently analyze the remotely sensed data into management relevant data such as percentage of green vegetation and end of year measures of cover, would help to provide data in near real-time. Lastly, the remotely sensed data needs to be accessible in a user-friendly web interface that displays the mapped vegetation amounts as well as key pasture statistics to increase the adoption of this data product.

Ranchers are seeking out data that better enables them to answer their own questions and assess their own management action so that changes can be made in future years. Actions such as purchasing Google Earth Pro licenses or contracting the services of range scientists demonstrates the desire of landowners to better informed managers of land and stock. Butterfield and Malmstrom (2006) demonstrated this want by concluding, most landowners said that they would increase the amount of money spent on this technology after their participation the study. Coupling private landowners with remotely sensed data products follows the recent trend pointed out by Burgess et al. (2007) and Dickinson et al. (2010) stating that that science has placed an emphasis on incorporating citizens in the policy and the scientific process. Incorporating citizens into the process by delivering remote sensing data products offer ways to improve management and grassland condition as well as the remote sensing science of grassland systems. Remote sensing technologies are well positioned to bridge citizens and the scientific community due to the richness in data, accessibility and its ability to highlight processes within and across ownership boundaries. The successes of such efforts depend on dependable and accurate data, a process of collaborative, ethical considerations and involvement in accessing remote sensing data and technology.

Bibliography

Burgess, J., Stirling, a., Clark, J., Davies, G., Eames, M., Staley, K., & Williamson, S. (2007). Deliberative mapping: a novel analytic-deliberative methodology to support contested science-policy decisions. *Public Understanding of Science*, *16*(3), 299–322. doi:10.1177/0963662507077510

Butterfield, H. S., & Malmstrom, C. M. (2006). Experimental Use of Remote Sensing by Private Range Managers and Its Influence on Management Decisions. *Rangeland Ecology and Management*, *59*(5), 541–548.

Coulloudon, B., Eshelman, K., Gianola, J., Habich, N., Hughes, L., Johnson, C., Pellant, M., Podborny, P., Rasmussen, A., Robles, B., Shaver, P., Spehar, J., Willoughby, J. (1999). Sampling Vegetation Attributes. Interagency Technical Reference, 171.

Dickinson, J. L., Zuckerberg, B., & Bonter, D. N. (2010). Citizen Science as an Ecological Research Tool: Challenges and Benefits. *Annual Review of Ecology, Evolution, and Systematics*, *41*(1), 149–172. doi:10.1146/annurev-ecolsys-102209-144636

Holechek, J., & Gomez, H. (1999). Grazing studies: what we've learned. *Society of Range Management*, *21*(2), 12–16.

Marsett, R. C., Qi, J., Heilman, P., Biedenbender, S. H., Watson, M. C., Amer, S., Weltz, M., Goodrich, D., Marsett, R. (2006). Remote Sensing for Grassland Management in the Arid Southwest. Rangeland Ecology and Management, 59(5), 530–540.

Myers, A. (2010). Camp Delta, Google Earth and the ethics of remote sensing in archaeology. *World Archaeology*, *42*(3), 455–467. doi:10.1080/00438243.2010.498640

Ortega-S., J. A., Lukefahr, S. D., & Bryant, F. C. (2013). Optimum Stocking Rate, Monitoring, and Flexibility. *Rangelands*, *35*(5), 22–27. doi:10.2111/RANGELANDS-D-13-00021.1

Rowley, R. J., Price, K. P., & Kastens, J. H. (2007). Remote Sensing and the Rancher: Linking Rancher Perception and Remote Sensing. Rangeland Ecology and Management, 60(4), 359–368.